Additive Manufacturing 45 (2021) 102058

Contents lists available at ScienceDirect

Additive Manufacturing

journal homepage: www.elsevier.com/locate/addma

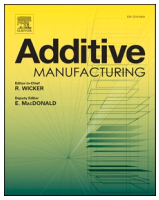

Review

In-situ sensing, process monitoring and machine control in Laser Powder Bed Fusion: A review

Ronan McCann [a,b,c,d,*], Muhannad A. Obeidi [a,b,c,d], Cian Hughes [a,b,d], E.Éanna McCarthy [a,b,c,d], Darragh S. Egan [a,e], Rajani K. Vijayaraghavan [a,b,c,f], Ajey M. Joshi [g], Victor Acinas Garzon [h], Denis P. Dowling [a,e], Patrick J. McNally [a,b,c,f], Dermot Brabazon [a,b,c,d]

[a] I-Form Advanced Manufacturing Research Centre, Ireland
[b] Advanced Processing Technology Research Centre, Dublin City University, Glasnevin, Dublin 9, Ireland
[c] National Centre for Plasma Science and Technology, Dublin City University, Glasnevin, Dublin 9, Ireland
[d] School of Mechanical and Manufacturing Engineering, Dublin City University, Glasnevin, Dublin 9, Ireland
[e] School of Mechanical and Materials Engineering, University College Dublin, Belfield, Dublin 4, Ireland
[f] School of Electronic Engineering, Dublin City University, Glasnevin, Dublin 9, Ireland
[g] Applied Materials Incorporated, 3050 Bowers Avenue, Santa Clara, CA 95054, United States
[h] Applied Materials Ireland Limited, Block A Maynooth Business Campus, Maynooth, Co. Kildare, Ireland

ARTICLE INFO

Keywords:
Additive manufacturing
Powder bed fusion
Process sensing
Machine control
Smart manufacturing
Selective laser melting
Electron beam melting
Industry 4.0
In-situ monitoring

ABSTRACT

Process monitoring and sensing is widely used across many industries for quality assurance, and for increasing machine uptime and reliability. Though still in the emergent stages, process monitoring is beginning to see strong adoption in the additive manufacturing community through the use of process sensors recording a wide range of optical, acoustic and thermal signals. The ability to acquire these signals in a holistic manner, coupled with intelligence-based machine control has the potential to make additive manufacturing a robust and competitive alternative to conventional fabrication techniques. This paper presents an overview of the state-of the art of in-situ process monitoring in laser powder bed fusion processes and highlights some current limitations and areas for advancement. Also presented is an overview of real-time process control requirements, which when combined with the emergent process monitoring tools, will eventually allow for in-depth process control of the powder bed fusion process, which is essential for wide-scale industrial credibility and adoption of this technology.

1. Introduction

Recently there has arisen a great interest in developing what is now referred to as "smart manufacturing" where process data from in-situ sensors, diagnostics or on- or at-line process monitoring tools are used to make autonomous decisions using machine intelligence. One branch of fabrication techniques making increasing use of these "smart" approaches in recent years is Additive Manufacturing (AM). The AM approach is an advanced manufacturing technique for the fabrication of metal, polymer, ceramic or composite parts which are formed layer-by-layer, ultimately forming a three-dimensional part with desired geometries and mechanical or other properties, as translated from a Computer Aided Design (CAD) file as discussed in [1]. While AM initially saw use mainly in rapid prototyping, it can be used indirectly in production, producing dies or patterns, or directly producing the parts themselves with a variety of commercially relevant materials. As such, it has become established in industry for the production of high-value or low-volume parts such as those found in the aerospace and automotive industries [2]. AM provides the ability to revise or customise parts with minimal adjustments to the production setup and supply chain [3], which can reduce waste or energy-consumption, making it a highly sustainable production method compared to conventional manufacturing approaches. Furthermore, it allows for complex topology-optimised structures, including bio-inspired designs [4], which can deliver superior part properties such as high strength-to-weight ratios [5].

Within AM, specific processes such as Powder Bed Fusion (PBF) are highly suited for the incorporation of in-situ or online sensing approaches. In PBF, a laser or electron beam is used to selectively melt polymer, metal or ceramic powders in a layer as defined by the operator

* Correspondence to: School of Mechanical and Manufacturing Engineering, Dublin City University, Glasnevin, Stokes Building (Room S117), Dublin 9, Ireland.
E-mail address: ronan.mccann@i-form.ie (R. McCann).

https://doi.org/10.1016/j.addma.2021.102058
Received 5 November 2020; Received in revised form 14 April 2021; Accepted 14 May 2021
Available online 21 May 2021

[6], as shown in Fig. 1. The part is then lowered and a fresh layer of powder coated on top of the previous layer, which is itself then selectively melted, with this layer-wise approach repeated to form an entire part of defined geometry [7]. Two sub-categories exist depending on the thermal source used to selectively melt the powder layer. Where a laser beam is used as the thermal source for powder melting, the technique is referred to as Laser Powder Bed Fusion (L-PBF), and where an electron beam is used, it is referred to as Electron Beam PBF (E-PBF). In the PBF process, the most important controllable parameters are beam power, beam scanning speed and hatching distance, and powder layer thickness, all of which can have a significant effect on the final part quality. To aid in understanding these effects, but especially to cope with the immense number of uncontrolled parameters, research is ongoing towards the integration of process sensors and monitoring tools to allow for detailed characterisation of the build process, and prediction of the properties of the subsequent produced part. Both machine diagnostics (laser power, gas flow, etc.) and process sensor returns (melt pool temperature, etc.) can generate a large volume of data, with sampling rates well suited for real-time process monitoring.

The incorporation of smart manufacturing approaches such as process sensing into AM, and specifically PBF, would allow for the optimisation of various part properties such as dimensional accuracy, porosity, surface roughness and mechanical properties. By combining data such as input parameters, process sensor signals and the characterisation of the final part, coupled with a system with learning and decision-making abilities, rapid optimisation of the finished part and processing conditions can be achieved.

To improve control of the AM production process, there is a great interest in the development of novel process sensors, improving existing sensing techniques and assessing which combination of process sensors is best for specific processes, materials or parts. Therefore, it is of vital importance to understand which sensors are applicable to specific quantitative and qualitative measurements during the build and how best to relate these to final part qualities. The resolution, accuracy and reliability of the sensors used must be understood, especially when the final parts are to be used in safety critical applications such as in the aerospace industry. Specific qualities such as surface finish or porosity can be detected by multiple types of sensors and such a holistic approach should be adopted where possible, with the correct selected process sensors running concurrently to gather larger, more reliable and representative datasets. This is particularly relevant where new AM processes or materials are being developed.

2. Defects in powder bed fusion

The PBF process can result in a number of part defects such as internal porosity, hot cracking, or the formation of the material balling on the surface of the part. These defects are often result from unsuitable or variations in the processing parameters during the build. This can result in an adverse effect on the final part quality and thus must be mitigated during the build if possible. Understanding the origins of these defects is therefore paramount to achieving optimal builds.

2.1. Surface and geometric defects

Outwardly visible defects present in pieces produced using PBF can be broadly categorised as either surface defects or geometric defects [8]. Of these geometric defects, those resulting in dimensional inaccuracy are the most immediately noticeable and problematic for PBF-based manufacturing. Depending on the extent of such defects, a piece may fall outside the tolerances required for its intended purpose rendering it unusable. Defects may be the result of low tessellation in the CAD data provided to the PBF machine [9] and are thus the result of user error, limitations in computational power or algorithmic error. Likewise, the fundamental limitations of the PBF apparatus itself can result in dimensional inaccuracies, whereby the geometric accuracy of a produced part is highly dependent upon the ultimate dimensional accuracy of the machine used [10]. Defects can also be the result of process-induced effects, such as thermal gradients [11] and residual stress [12]. Wegener et al. found that the most important source of these error effect is by far are thermal in nature, which may bring the part several millimetres out of the intended geometry [13] Thus, the process

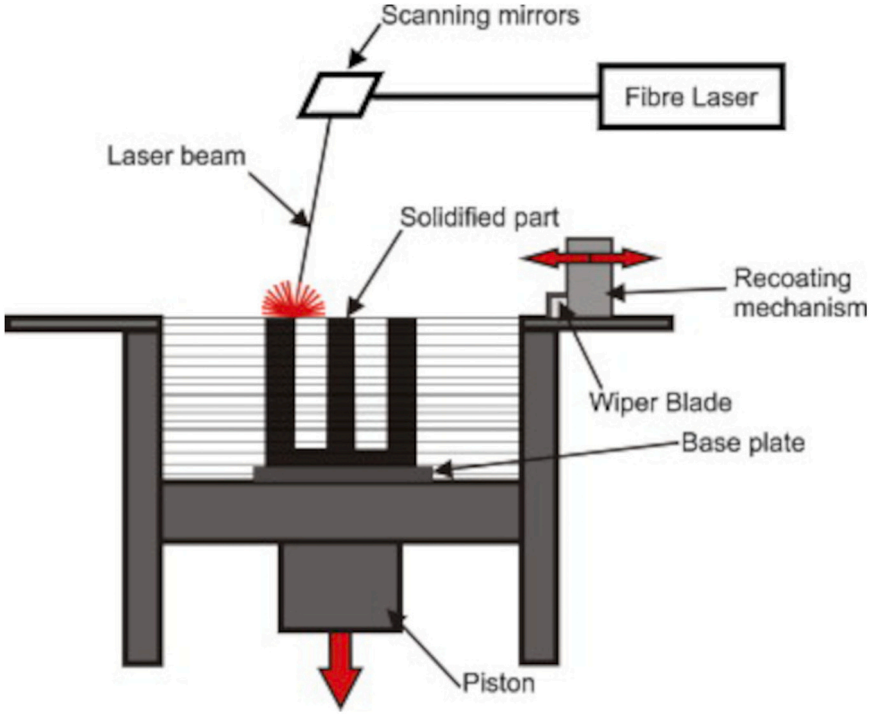

Fig. 1. Schematic of the PBF process.
Reproduced from [7].

parameters most likely to cause geometric defects are primarily those associated with the source of thermal energy source, i.e. the laser or electron beam parameters.

Surface defects resulting from the PBF process can be categorised to encompass surface oxidation, deformation, roughness and balling [8]. Oxidation occurs when the material comprising the piece reacts with atmospheric oxygen present during the build. It has been found that the oxidation behaviour of PBF produced pieces is similar in mechanism to that in conventionally manufacturing processes involving the melting and solidification of material [14]. The use of an inert gas atmosphere during processing can limit or mitigate some of these oxidation effects. Surface roughness defects are a major factor in the fatigue and crack nucleation of where small surface peaks and valleys facilitate the initiation and subsequent propagation of cracks through the piece [15–18].

Finally, balling – the formation of solidified balls of material on the part surfaces after melting – often occurs where the powder used in a PBF process has high surface tension in the liquid phase. This surface tension leads to poor wettability, leading to the formation of rough, bead-like solids and is often found when the melting-phase occurs at a relatively low energy density, generally disappearing with increased laser power or decreased scan speed [19,20]. Li et al. demonstrated this effect of scan speed (shown in Fig. 2) for stainless steel 316L parts [21]. These balls can form highly rough surfaces, or pores between two or more balls when in contact. Extreme balling can interfere with the powder recoating step in PBF process, resulting in the next layer having an uneven powder coating which can lead to compounding further defects or geometric inaccuracies later in the build.

2.2. Sub-surface defects

Sub-surface defects, such as porosities or cracks can be commonly present in parts produced via PBF. Edwards et al. [22] found that porosity has a significant impact on the fatigue characteristics and crack propagation behaviour through a part and is thus a crucial factor to control during the build process. Porosities can form within individual layers, between adjacent layers (which can contribute to delamination of layers), or on the surface of parts. Kasperovich et al. [23] examined the formation of porosities in TiAl6V4 parts produced via PBF. Parameters such as laser scan speed and beam diameters were found to be the most crucial parameters to control for reducing the formation of pores (Fig. 3). Where insufficient or excessive scan speed and laser power were used, porosities were formed through two separate mechanisms. Incomplete melting of the powder as a result of low power or high scan speed resulted in the formation of narrow crack-like voids. Conversely, at high power or low scan speeds, the “keyhole effect” was seen whereby material in the meltpool was vaporised resulting in a bubble-like cavity upon solidification. This overmelting of the powder bed has a significant effect on the incorporation of unmelted powder, formation of voids and

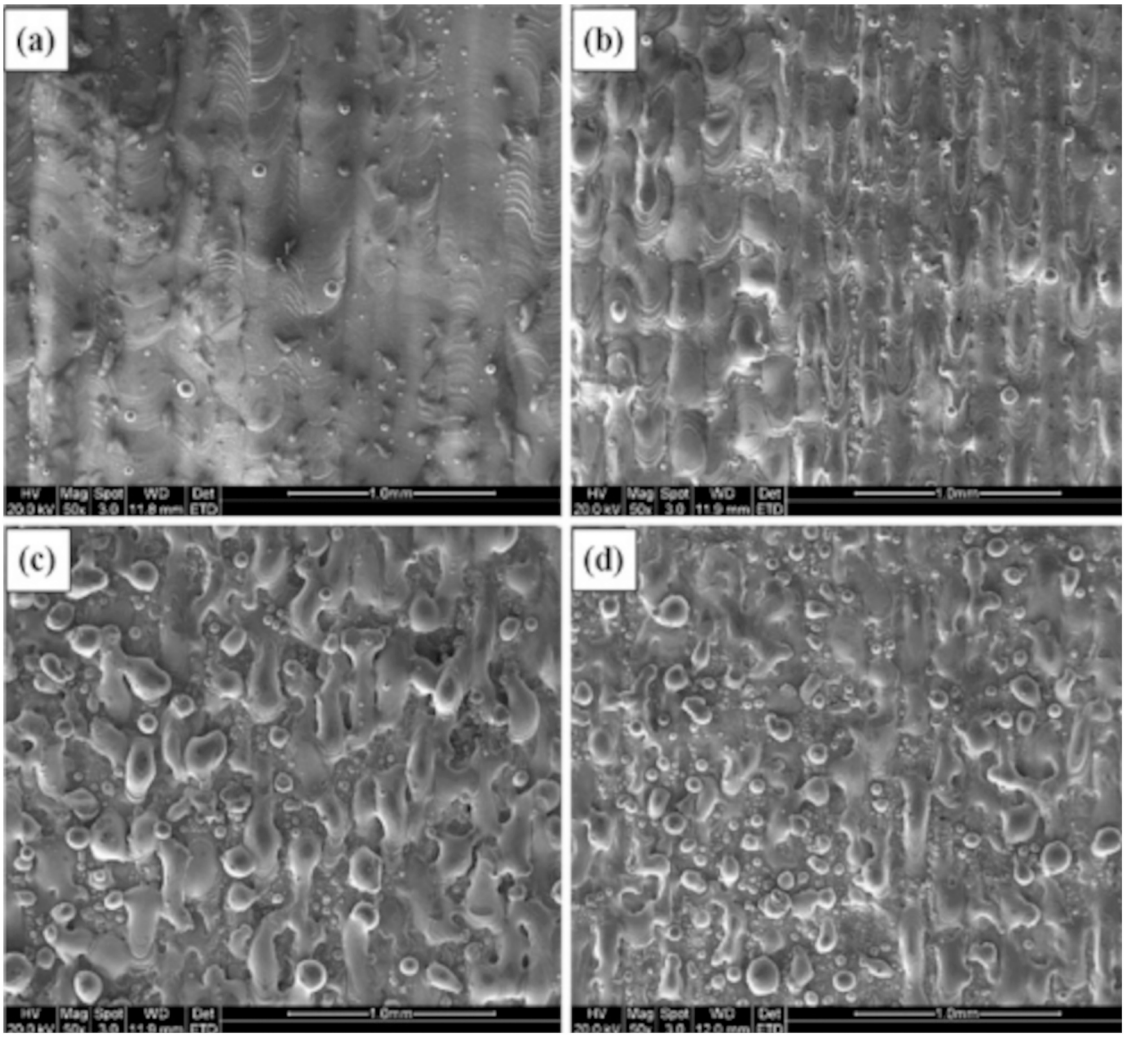

Fig. 2. Balling behaviour of stainless steel 316L in the PBF process. The process parameters used were a laser power of 190 W, hatch spacing of 150 μm and laser scan speeds of (a) 50 mm/s, (b) 400 mm/s, (c) 600 mm/s, and (d) 800 mm/s.
Reproduced from [21].

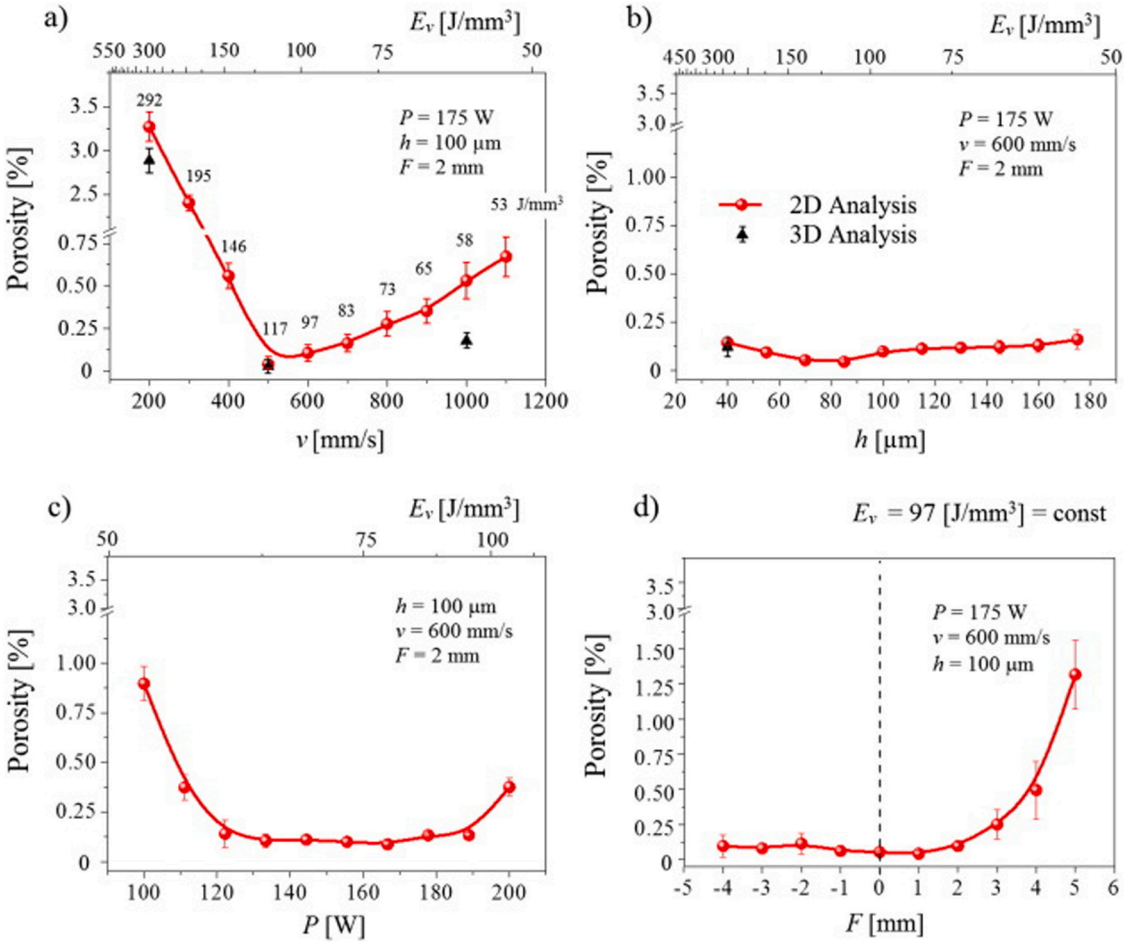

Fig. 3. The effect of PBF process parameters such as (a) scan speed, (b) hatch spacing, (c) laser power, and (d) focal distance on part porosity. Reproduced from [23].

porosities, and ultimately the final density of the part [24].

The PBF process can often have large thermal gradients present during the build resulting in the formation of residual stress within the part. These are highly dependent on both the process parameters used and the material being formed. These residual stresses can lead to internal or external cracking where the residual stress state exceeds the tensile strength for a particular part. Extreme examples of this result in the delamination of individual layers or between individual laser scans, such as that shown in Fig. 4. Scan strategy can play a significant role in mitigating this, such as when each layer is processed at varying angles to their adjacent layers, or by ensuring there is sufficient melting of each layer. Louvis et al. [7] examined the effects of scan strategy for the fabrication of parts using aluminium alloys (6061 [AlMg1SiCu] and AlSi12), with extreme delamination seen where laser power was insufficient.

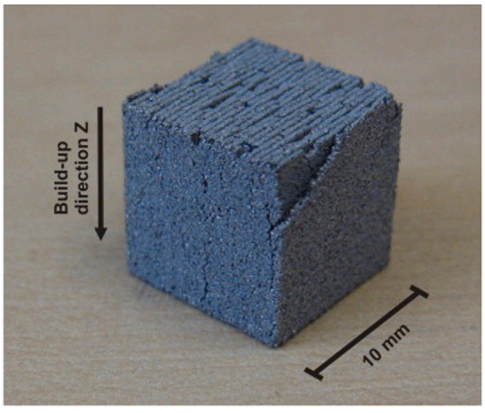

Fig. 4. Delamination shown at the surface of an aluminium alloy 6061 (AlMg1SiCu) specimen. Selected hatch distance of 0.4 mm was larger than the molten track width resulting in delamination.
Reproduced from [7].

3. In-situ process sensing

Process sensing is commonly used in many advanced manufacturing processes such as the chemical, pharmaceutical and semiconductor manufacturing fields. These sensing approaches focus on the incorporation of sensors capable of recording acoustic, thermal, optical or other signals such as those normally monitored within biological systems [25] and has been noted as a key enabling technology for AM processes such as PBF, and manufacturing at-large [26]. Table 1 presents a summary of the in-situ sensing approaches used in PBF.

3.1. Acoustic techniques

Acoustic sensing in PBF measures either induced sonic or ultrasonic waves in the part, such as those produced as the laser is in operation or rely on transducers to impart sound waves into the sample. As these waves propagate through the part, the transmitted or reflected intensities can be used to determine a number of part properties. To date, two primary techniques for acoustic-based sensing have been applied in PBF processes: Ultrasonic Testing and Acoustic Emission Spectroscopy.

Table 1
Overview of reported in-situ process sensing approaches in PBF.

Principle	Coaxial	Recognisable type of defects	Vertical size [um]	Horizontal size [um]	Ref.	Notes
Ultrasonic Testing	–	Porosity	40	–	[27, 28]	Qualitative, but potential for calibration against known porosities.
Acoustic Emission Spectroscopy	–	Balling, Overheating, Porosity, Cracking	–	–	[29, 30]	More suited for qualitative process monitoring.
Optical Imaging	On/Off	Powder Bed Irregularities, Overheating	–	–	[31, 32]	Can be used for thermal measurements depending on detector.
Optical Emission Spectroscopy	On/Off	Overheating, Porosity	–		[33]	Commonly used in other advanced manufacturing techniques such as plasma deposition.
Optical Tomography		Balling, Surface Roughness, Dimensional Accuracy, Powder Bed Irregularities, Lack-of-fusion defects	–	–	[34, 35]	Suitable for sub-surface defect detection.
X-Ray Tomography		Porosity	–	–	[36, 37]	Less developed for in-situ AM applications than other tomographic methods.
Optical Coherence Tomography	On/Off	Porosity	20	50	[38]	Can examine powder bed, core part regions or bending defects on part. Limited to surface analysis.
Pyrometry	On/Off	Overheating	–	–	[39]	Suitable for single or multiple point measurements in the build area. Total scan area depending on optical setup.
Infrared Imaging	On/Off	Overheating	–	$> 600 \times 600$	[40]	Can be scaled to entire build areas with reduction in spatial resolution.

3.1.1. *Ultrasonic Testing*

A widely used non-destructive testing method for determining the presence of sub-surface defects is Ultrasonic Testing (UT). UT relies on the conduction of ultrasonic waves through a part and records a time-resolved acoustogram of the reflected or transmitted waves. UT is a common non-destructive test in industrial contexts [41], such as in the aerospace industry where it is used for fatigue testing during a part lifecycle. Aleshin et al. noted that UT would have strong potential as a metrological tool for AM produced parts, specifically when working with materials of alloys susceptible to the formation of large voids or porosities [42].

Offline metrology can rely on pulser/receivers or phased arrays of ultrasonic transducers [43] or the use of lasers for the generation of ultrasonic waves [44]. For in-situ monitoring, an ultrasonic transducer is mounted under the build plate, and ultrasonic waves transmitted through the build plate into the part, and the ultrasonic wave reflection recorded, often with the use of a combined pulser/receive unit for simplicity of the experimental setup.

As an online process tool, Rieder et al. [27] demonstrated in-situ monitoring of a PBF process using a single UT transducer mounted underneath the build platform during part fabrication which was capable of determining the presence of voids with simple geometries. Building on this work, Rieder et al. [28] demonstrated that porous layers, which were induced in an Inconel 718 part by varying the laser power during the build, were detectable using in-situ UT. Fig. 5 shows the recorded ultrasonic signal and corresponding X-Ray Computed Tomography (CT) image of a part fabricated via PBF. The variation of laser power for certain layers has induced a number of porosities, seen both on the CT image and via ultrasonic reflections. As the ultrasonic wave passes into a more porous layer, waves are scattered and reflected, and are recorded by the detector [28], which was also mapped to individual layers of the build itself.

Given the complexity of CT compared to UT, this highlights the ability of a more conventional in-situ process tool to acquire data on part porosity. These detected waves are characteristic to each ultrasound unit and setup and can be calibrated through the production of parts with known internal porosities and voids, or by post-process analysis of part porosity through sectioning micro-CT analysis. UT has the advantage to

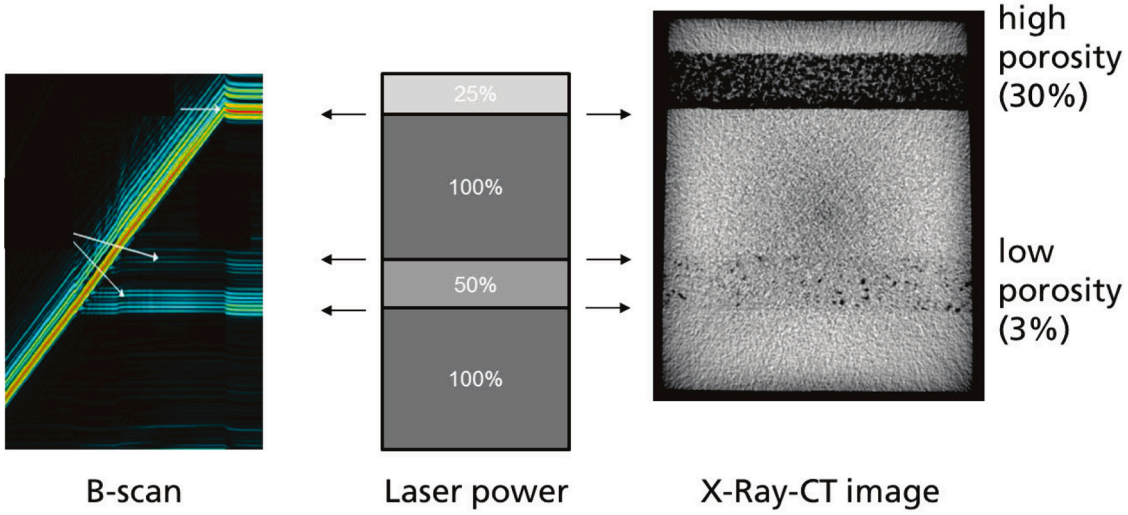

Fig. 5. An in-situ ultrasonic scan and corresponding X-Ray CT image of an Inconel 718 part. Porosity was induced in the sample by reducing the laser power at specific points in the build. This porosity was evident via UT by increased ultrasonic reflections within the porous layers.
Reproduced from [28].

be used both in-situ as an online process monitoring tool, and offline as a QA tool, allowing correlation of on- and offline data. UT can also be multiplexed with multiple transducers to allow for large area acquisition, though the data analysis becomes increasingly complex, and presents a potential area for artificial intelligence in AM data analysis.

3.1.2. Acoustic Emission Spectroscopy

Through examination of the acoustic emission during a PBF process, it has been possible to detect defects such as cracking, delamination, excess surface roughness, or the formation of pores. Ye et al. [45] reported in-situ acoustic monitoring of PBF of 304 stainless steel using a

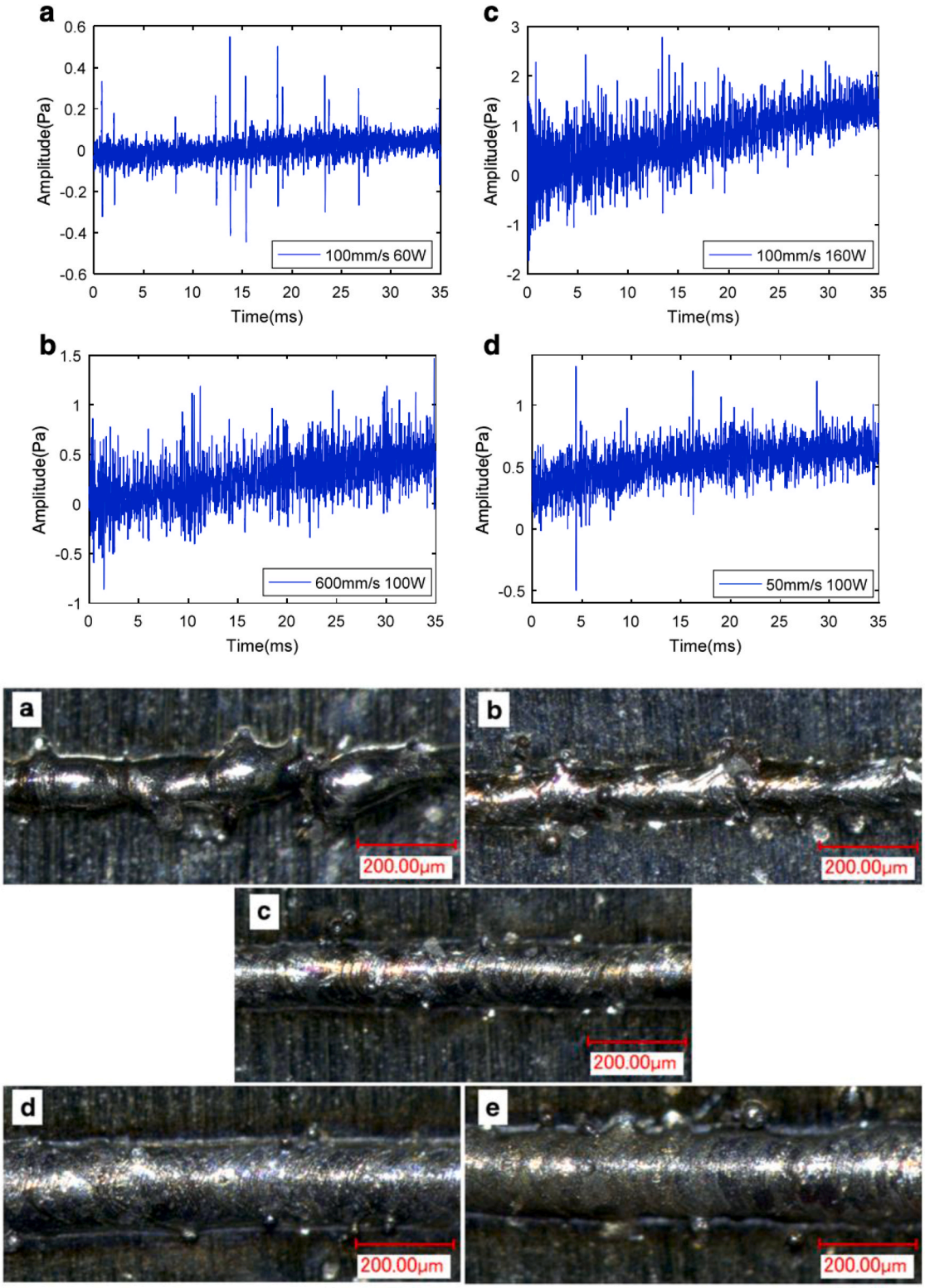

Fig. 6. Acoustic Emission signals and corresponding micrographs for (a) balling, (b) slight balling, (c) normal and (d) slight overheating, and overheating, (shown in (e) for comparison).
Reproduced from [45].

microphone with a frequency response from 0 to 100 Hz. Fig. 6 shows the recorded acoustagrams and corresponding optical micrographs. Their acoustic monitoring system was able to distinguish between 5 different defect states: balling of material on the surface, slight balling, normal deposition, slight overheating, and overheating.

Smith et al. [29] used spatially-resolved Acoustic Emission Spectroscopy (AES) for in-situ inspection of part porosity, during PBF. While the technique does not yet allow for accurate quantification of defects, it can be used to acquire qualitative data about part quality during the build process. As the recorded signals are quite complex with multiple factors effecting small to large changes in overlapping frequency spaces, artificial intelligence and machine learning is often employed for analysis of these signals.

Shevchik et al. [30] utilised Acoustic emission spectroscopy AES and artificial neural network analysis to categorise samples (poor, medium, and high quality) as defined through ratings of part porosity. The system also employed a laser Bragg grating as the acoustic sensor element, which is well suited to high noise environments. The algorithm categorised these defects with an approximately 80% accuracy to the correct category of part. As acoustic signals resulting from the PBF process are quite complex, this result highlights the current state of the art of machine learning approaches in simplifying acoustic emission data analysis.

3.2. Optical techniques

Imaging approaches towards process monitoring are attractive option given their ease of use, ability to be located at a distance from the build environment and ease of incorporation into existing systems [46]. Conventional optical or IR imaging provides information on the surface of the part or powder bed, while tomographic methods can provide information regarding the internal structure of parts during fabrication.

3.2.1. Optical Imaging

In-situ optical monitoring techniques are based on visible or near-infrared imaging, with analysis of the data obtained from this straightforward method allowing detection of defects during part production [47]. In one approach, Craeghs et al. investigated powder bed monitoring during the PBF process via optical imaging [31]. This technique allowed for monitoring of the powder layer recoating process and any disruptions in the powder bed, shown in Fig. 7. Disruptions in the powder bed may be as a result of damage to the recoating blade, movement of the part on the build tray, or issues with powder supply. As the recoating process has significant impact on the resultant part quality, this form of optical sensing has immediate implications towards process monitoring. Zhang et al. demonstrated the use of digital fringe projection for in-situ optical monitoring in a PBF process [48]. The system records data on the surface of the powder bed and the part top surface in a layer wise manner. Though the authors note that setup of the system is non-trivial, due to the optical scattering behaviour of the part and powder bed, the system presents a potential optical route for powder bed and part monitoring during the build process.

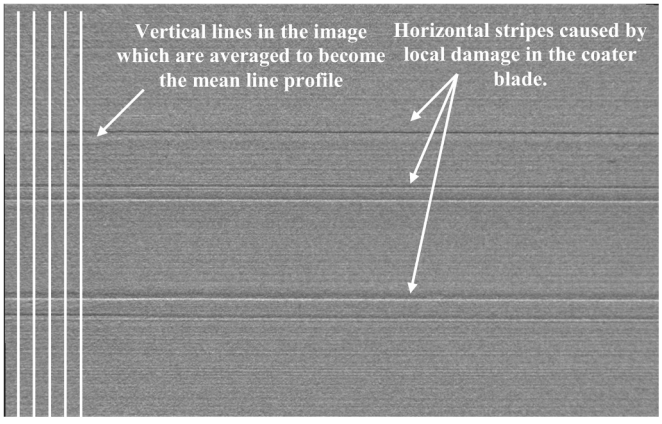

Fig. 7. Optical camera image of the powder bed surface after powder spreading with a worn recoater blade.
Reproduced from [31].

Examination of the meltpool via in-situ optical imaging is a highly active area of investigation. This is unsurprising considering the amount of information on the thermal behaviour of the process that can be extracted. Optical imaging can be used to estimate the melt pool temperature in a similar method to thermal imaging, though not requiring IR-specific sensors, instead exploiting the NIR spectral range of commercial optical cameras. Yadroitsev et al. [32] demonstrated this technique using an on-line CCD camera to monitor the melt pool for Ti6Al4V. Using the solidification temperature as a reference point, the optical intensity could be used to estimate the temperature of the meltpool, allowing a correlation to the input parameters such as laser power, irradiation time, and scanning speed.

Though getting precise thermal measurements from optical examination can prove difficult, indirectly examining irregularities in the meltpool can yield significant information. Yang et al. utilised a high-frame rate camera for detection of melt-pool irregularities and splatter of and Inconel 625 process [49]. The high-frame rate of the imaging system was capable of rapid detection of overmelting of the powder bed and for statistical process control analysis, and significant scope for adaptive process control. Criales et al. utilised in-situ video imaging to examine meltpool behaviour during PBF of nickel alloy 625 [50]. The system was capable of detecting overmelting, and the data gathered by the system on the heating and cooling rates was also noted to be useful to validate models of the microstructure of produced parts. Similar work using 2D finite element modelling showed the capability to extend meltpool imaging towards modelling of part properties such as density [51].

Repossini et al. examined the behaviour of a maraging steel meltpool using high-speed off-axis in-situ imaging [52]. While the system was capable of detecting splatter, efforts to quantify process errors in the heat affected zone proved difficult with the off-axis setup. Despite this, the authors note that there is scope for this approach in conjunction with on-axis monitoring where complex part geometries are present in the build.

Mazzoleni et al. examined both visible and infrared wavelengths using a CMOS imaging camera and found it was possible to more accurately capture information relating to the melt pool, plume dynamics and exploit the dynamic range of CMOS in the IR region. This highlights the choice of wavelength and hardware for in-situ imaging applications especially where high resolution is required for real-time control [53].

The application of Convolution Neural Networks (CNNs) to infrared imaging techniques can yield significant benefits allowing for real-time process monitoring [54]. The CNN required for real-time monitoring using infrared imaging was significantly less complex in comparison to that required for real-time monitoring using visible wavelength imaging [54,55], therefore requiring less powerful computing equipment and providing quicker calculations. This once again highlights wavelength range selection in imaging as highly important in real-time applications, especially closed-loop control where rapid corrective action may be required.

Even with advances in processing speed, the application of CNNs have mostly been limited to process monitoring due to the time required between data acquisition, processing and an action being taken [55]. The use of high-speed Field-Programmable Gate Arrays or Application-Specific Integrated Circuits for data acquisition, coupled with efficient CNNs have the potential to allow the use of readily obtainable data to predict a wider variety of properties in real-time and for closed-loop process control.

Looking beyond optical or near-optical imaging, ultrafast x-ray

imaging has been applied in the examination of the fusion mechanism [56,57] and melt pool irregularities [58] in PBF. The use of in-situ x-ray imaging allows for high spatial resolution, and initial results show potential as a possible method for increasing the fundamental physical processes occurring in PBF processes. However x-ray imaging remains an unexplored avenue for real-time process control.

3.2.2. Optical Emission Spectroscopy

Optical Emission Spectroscopy (OES) has been widely used for monitoring a range of plasmas and plasma processes for research and industrial applications. OES data collected from a plasma has an abundance of information and can be used for a broad range of process control, process monitoring and troubleshooting applications [59]. OES has also attracted enormous interest as a powerful means to characterise laser induced plasmas, and to investigate the consequent laser material interactions in laser processes such as welding or nitriding [59].

Early work by Szymanski et al. using OES analysis of CO_2 laser induced welding plasmas for titanium and stainless steel found that the plasma is in a state of thermodynamic equilibrium [60]. With this assumption they estimated the electron temperature using the ratio of the emission line intensities and the electron density from Stark broadening of atomic lines [61,62]. Many studies have been performed to explore the possibility of using OES as a real-time monitoring tool for laser induced plasma processes. Ancona et al. carried out real-time electron temperature calculation using Fe(I), Cr(I) and Mn(I) emission lines from stainless steel welding plasma and the temperature variation was correlated with the formation of welding defects [63]. Similarly, real-time monitoring of both process stability in laser hot wire cladding and the quality of the arc welding were also performed using OES [64,65]. In-process OES investigations of laser-induced aluminium alloy 5083 welding plasmas found a correlation between the spectral features and the formation of oxide layers on the surface of the welding seam, which had originated via the vaporisation of alloying elements and defective gas shielding [66].

In a different study, Nasser et al. employed OES to investigate laser nitriding of titanium [67]. As part of developing a fast and accurate method for the real-time composition analysis, Song et al. incorporated the OES technique in order to monitor the direct metal deposition (DMD) process of pure chromium and H13 tool steel materials, and their OES-based analysis was capable of predicting Cr compositions with a prediction error of 0.06% [68]. Though the laser welding and nitriding processes vary significantly from the PBF process, nevertheless it serves to highlight that there is significant body of work on the laser plasmas from materials with which to compare data from AM processes. These works combined with existing databases such as the National Institute of Standards and Technology (NIST) Atomic Spectra Database [69], can serve as reference material and starting points for investigations into OES in AM processes.

Although OES has been used in blown-powder AM processes, limited reports are available on its application to PBF-based AM processes. As part of the development of a real-time communications architecture for metal PBF process, Dunbar et al. demonstrated real-time measurement of the build process using OES [33]. They used an Ocean Optics HR2000-ES spectrometer mounted at a fixed location inside the build chamber to monitor the optical emissions and to measure the effect of the defocussing parameter in a 3D Systems ProX 200 machine [33]. In this work, they were able to provide comparisons of emission spectra by isolating spectrometer measurements at different defocus positions of the PBF process laser beam [33]. As a continuation to this work, Dunbar and Nassar conducted real-time OES monitoring of PBF AM processing of an Inconel-718 component build-up in a 3D Systems ProX 200 tool [70]. They developed an off-axis dual-spectral sensor based on line-to-continuum measurements of Cr I emissions around 520 nm and found that these emissions can be correlated with the defects within PBF AM-manufactured components [70].

In-situ OES has been employed to monitor the PBF process with 304L stainless steel in a home-built PBF system (Fig. 8), as reported by Lough et al. [71]. While the implementation of OES for the PBF process is somewhat challenging, due to the presence of the galvo-scanner guided laser beam as well as the moving melt pool, they introduced spectrometer optics into the laser beam path using a beamsplitter which was on-axis with the galvo-scanner and PBF laser [71]. Using the in-situ OES analysis they could correlate the calculated plume temperature with the melt pool size and found the dependence of the chamber type and pressure on the PBF process (Fig. 9).

Lough et al. demonstrated that the OES can be used to provide useful feedback to the PBF process for process monitoring and part validation, if it is implemented in-line with the laser path in a commercial system [71]. Very recently, Rao et al. demonstrated the implementation of a multispectral optical emission sensing technique together with a graph theoretic signal analysis technique for detection and identification of porosity in PBF of nickel alloy 718 [72]. Using this approach they predicted the porosity on a layer-by-layer basis with ~90% accuracy in a computational time of < 0.5 s [72]. In-situ OES measurements have also been shown effective for the prediction of properties such as porosity [72], flaw density [73], and overall part quality [73,74]. Although there are many studies showing the potential of the OES technique for laser-induced plasma characterisation, more research needs to be focused on the implementation of OES for real-time monitoring of PBF processes in order to investigate the effectiveness of this technique for a range of materials, defects, laser parameters, varying geometries, etc. in commercial systems.

3.3. Tomography

It is possible to yield tomographic data of parts produced via PBF by building a 3D representation comprised of many 2D cross-sectional images taken during the build process. The nature of PBF is complementary with this tomographic approach as the piece can be characterised by optical or other imaging approaches in a layer-wise manner. Optical tomography at visible wavelengths has been demonstrated for detection of lack-of-fusion defects during the melting process [34]. This approach yielded high-resolution data that was applied towards automatic defect detection in the produced parts.

Ubiquitous in many fields including AM [36,37], micro X-ray Computer Tomography (μ-CT /XCT) is a common metrological technique for post-fabrication characterisation, but can suffer from large variation in quality between scans [75]. Townsend et al. developed a technique for the extraction of areal data from volumetric XCT scans of PBF produced parts [76]. As the production of internal features is one advantage of AM over conventional manufacturing, this new XCT technique has potential for assessment of the internal surfaces and simplifying the quality assessment of these parts.

This technique can also be applied as an in-situ sensing approach and has been demonstrated in the identification of defects such as lack-of-fusion, porosity and balling during the PBF process [37,77]. Recently, it has been found that combining optical tomography with infrared tomography can result in a technique capable of detecting defects with an accuracy comparable to that of μ-CT [35]. This combined technique has the potential to be a lower-cost alternative for subsurface defect detection with significantly lower hardware requirements than μ-CT.

Another tomographic approach suitable for in-situ monitoring is Optical Coherence Tomography (OCT). OCT is based on a technique referred to as Coherence Scanning Interferometry (CSI), wherein constructive and destructively interfering reflected light is used to topographically and optically map a surface with repeated CSI measurements, allowing a full picture of the part as it is formed. OCT has found increasing applications in AM fabrication processes and PBF in particular [38]. By taking repeated CSI measurements, a tomographic view of the piece can be built up for analysis. The optical setup for OCT uses a laser interferometer which is set up to be optically in-line with the PBF laser. This allows for a simpler optical setup, while also having the

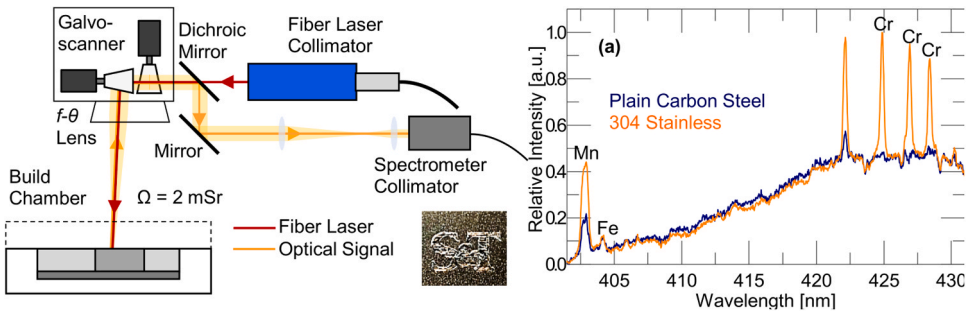

Fig. 8. (a) Schematic of the optical components of the PBF system with spectrometer inserted into the beam path, and (b) variation of optical emission signals from plain carbon steel and stainless steel.
Reproduced from [71].

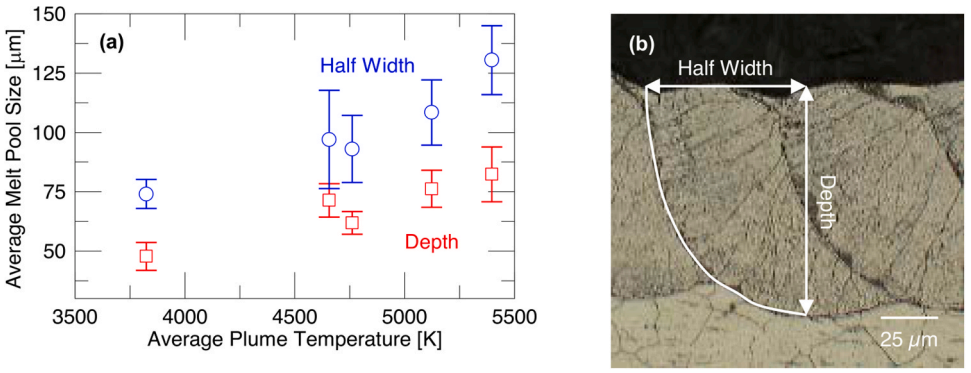

Fig. 9. Correlation of melt pool size to average plume temperatures during single layer processing.
Reproduced from [71].

functionality of examining the laser melt process during part fabrication.

OCT can be considered a light-based analogue to ultrasound, and offers wavelength-encoded depth information of a sample with 1–20 μm axial resolution [78]. This imaging technique is the standard of care in ophthalmology, where it is used for corneal and retinal imaging. Neef et al. [78] demonstrated OCT in a PBF process allowing for inspection of the powder bed prior to melting, inspection of the melt pool and inspection of the produced part surface in each layer. Non-uniformity in the powder bed and defects of approximately 50 μm were seen after processing (see Fig. 10) highlighting the ability of the technique to detect fine defects in the build process.

One study found OCT to be comparable to confocal microscopy and X-ray μ-CT when examining parts produced via PBF, however the authors note significant uncertainty and disagreement between techniques

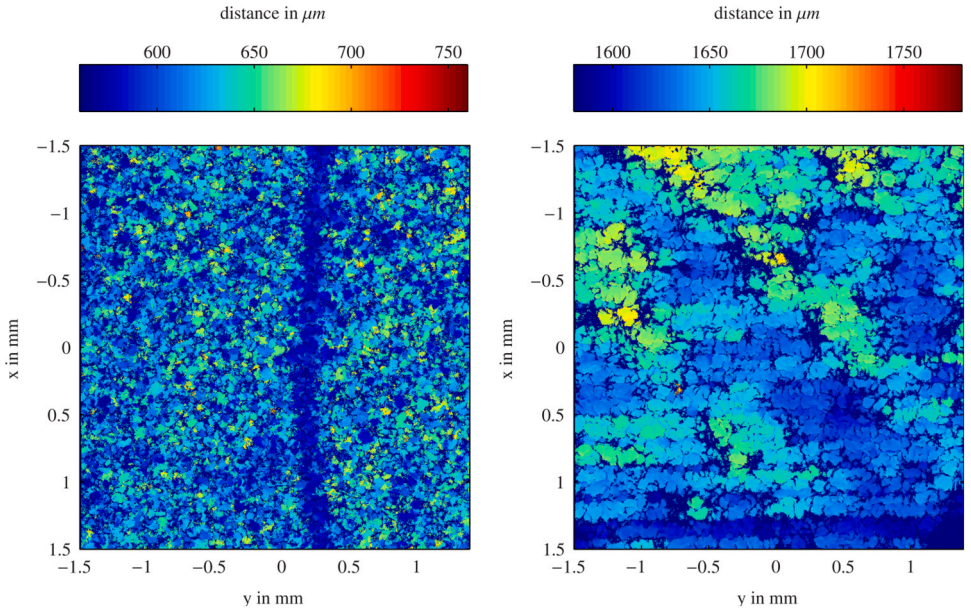

Fig. 10. Surface profile scans of powder material and a PBF produced structure as recorded using OCT.
Reproduced from [78].

when assessing topographical details [79]. Despite this uncertainty, OCT was found to offer the potential for sub-micrometre resolution, allowing for the more accurate identification and assessment of defects. In-situ OCT testing has been shown to have similar capabilities to μ-CT methods with the additional benefit of allowing for the identification of dross and measurement of layer roughness [80], a measure correlated with overall part quality.

3.4. Thermal techniques

Thermal measurement is a common process non-contact sensing approach in advanced manufacturing laser processes such as welding, thermal hardening, cladding and more recently for both L-PBF [81] and E-PBF [82,83]. By measuring the thermal radiation emission from the powder bed under laser irradiation, it is possible to gain insight into the thermal gradients present the in the PBF process which can have significant influence in final part properties such as microstructure.

3.4.1. Absolute vs. radiant temperature

Non-contact IR thermal measurements rely on radiant thermal emission, which can vary significantly from the absolute temperature of the emissive body itself. This presents a significant potential source of error when accurate temperature measurement is required for modelling or quantitative determination of physical processes occurring during the build.

A key physical parameter for IR measurements is the emissivity of the radiative material, in the case of PFB, the powder bed, meltpool and solidified part. The emissivity of a material is highly dependent on both temperature and wavelength, surface morphology [84] and the oxygen content of the feedstock, and can change when the material is subjected to multiple heating cycles, such as through powder recycling in PBF [85–87]. This clearly shows the importance of accurately quantifying the emissivity of the feedstock material though all stages of use, especially when powder is used through multiple cycles, prior to determination of the temperatures present. Zueco et al. presented a method to estimate the emissivity over relevant temperature ranges using a numerically solved network simulation [88]. This approach would allow for more accurate determination of the temperatures present in the PBF process, and also serves to highlight the use and applicability of novel modelling techniques when approaching problems such as emissivity in the PBF process.

Rodriguez et al. examined the fundamental difference between absolute and radiant temperatures present inside an Ti6Al4V E-PBF process [84]. A blackbody radiator was used to calibrate the IR system, and a model was developed for the powder emissivity, which was then compared to experimentally determined emissivity using a blackbody radiator which had a 4% standard deviation when compared to the experimental thermocouple data. Ultimately a difference of approximately 366 °C between the uncorrected and corrected radiative temperatures (1038 °C vs. 672 °C) was seen when the IR thermography was corrected to account for emissivity during the E-PFB process. This highlights that radiative and real temperature measurements can vary significantly but through diligent modelling or measurement of the emissivity, and knowledge of the process, and calibration of sensors, can ultimately be corrected for. The authors also note that the model they present can be adapted to other AM processes where radiative thermal measurements are being taken. Work by Hooper compared IR imaging and thermocouple measurements, demonstrating another potential route towards quantitative calibration of thermal measurement equipment in PBF [90].

Thermal measurements in PBF are generally surface-based, and the thermal gradients between layers in a PBF build can have significant impact on the ultimate part properties. Williams et al. examined this using IR imaging, which were calibrated against thermocouple measurements to allow accurate determination of real temperatures [89]. The inter-layer cooling time, defined as the time between an area being scanned by the laser from layer-to-layer, was seen to have influences on microstructure formation, porosity, and melt-pool size. The authors note that knowledge of the surface temperatures is required when high confidence in consistent microstructure and part density is required for L-PBF produced components.

Other process conditions can significantly interfere with the measurement of the powder bed. Laser plume and plasma emissions, splatter ejection and ambient gas pressure and flow can have an impact on the IR emission and thus contribute a source of error to thermal measurements. Despite all this, the examination of the relative temperature differences present in a build, or from build-to-build, would still allow for statistical process control without requiring accurate calibration of the IR sensor, by examining variations in thermal emission, or thermal emission from unexpected areas of the powder bed.

Of the reports to date on thermal monitoring of PBF processes, most utilise either IR imaging or pointwise pyrometry, and there is significant differences in the data acquired between these two techniques.

3.4.2. Pointwise pyrometry measurement

Photodiode pyrometers are widely used in research and industry. They detect light emitted from the melt pool and convert it into an electrical signal which is proportional to the light intensity and is thus characteristic of the melt pool emissivity and behaviour [91]. This emissivity is highly individualised to the feedstock powder composition and size, and thus sensors must be calibrated prior to quantitative measurements being made. Despite this, even relative build-to-build measurements can allow for qualitative measurement of the reproductivity of a PBF process and allow for error detection. In contrast with thermocouples, pyrometers provide more flexibility for non-contact measurement which is necessary in the dynamic PBF process. However, pyrometers may have higher hardware or integration costs than some other techniques such as IR camera imaging depending on the resolution or thermal accuracy requirements in the process [92,93].

Mahato et al. [39] used the IR intensities recorded from two pyrometers fitted on a PBF machine for the prediction of part quality. The PBF machine was fitted with two pyrometers which detect the light emitted from discrete areas of the melt pool within the range of 1500–1700 nm. This dual pyrometer arrangement allows for investigation of both temperature at the laser spot, and the temperature gradient in the surrounding powder or meltpool. In a similar arrangement, Pavlov et al. [94] developed their original bi-colour pyrometer setup to measure the melt pool temperature in PBF for a range of the main processing parameters including layer thickness, hatching distance and scanning strategy. Despite using arbitrary units to display the pyrometer data of the temperature, the study produced very interesting results which help to understand the input thermal distribution, and effect of scanning strategy, shown Fig. 11. Significant variation in the signal was seen as a function of parameters such as hatching distance, or powder layer thickness which allowed for application of this online monitoring system towards part quality control.

3.4.3. Thermal imaging

Several studies have been carried out using both cameras and optical sensors to investigate thermal dynamics within additive manufacturing processes such as PBF and Direct Energy Deposition (DED) [40,95–99]. Berumen et al. [40] used the arrangement shown in Fig. 12 to record the melt pool geometry and the mean radiation intensity emitted by means of a 10 kHz camera and a photodiode.

This arrangement was first patented and licensed by Concept Laser [100] and later was developed and brought to industry in collaboration with KU Leuven. Another similar arrangement was also adopted by Clijsters et al. [101] and is under development for the real-time monitoring and detection of when melt breakage or material discontinuity occurs in AM process. This setup uses a high-speed CMOS camera to capture images within a wavelength range of 780–950 nm, below the laser wavelength of 1070 nm. The melt pool information is then

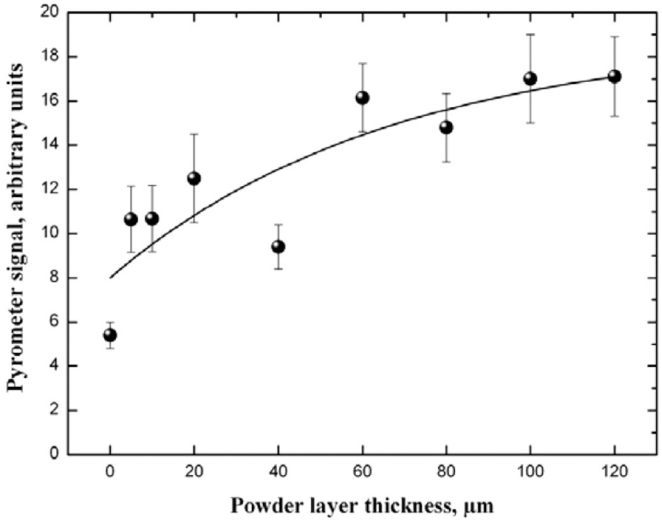

Fig. 11. An acquired pyrometer signal versus powder layer thickness. Reproduced from [94].

converted into a surface map corresponding to variations relative to a baseline. Fig. 13 shows an example of an acquired algorithmic mapping, and the corresponding microscope images for a AlSi10Mg part. The pores can be seen on both the computed xy-map the microscope image, and are a result of melt pool variation, thus demonstrating the system is capable of defect detection. In this approach sensitivity and accuracy of these maps is highly dependent on the data processing algorithm, is less sensitive to smaller defects and can result false positives where simple pixel thresholding is not robust enough to discriminate meltpool variation. Furthermore, there appear mismatches between the mapped pore locations and those visible under microscopy which was attributed to polishing of the specimen prior to imaging. Ultimately, the authors note that while proof-of-concept for this approach has been achieved, further work is required to validate and increase the robustness of this technique.

Heigel et al. examined the effects of laser parameters on melt pool geometry and temperature in a L-PBF machine [99]. A high-speed (1800 frames per second) sensor was used to capture the radiation in the range of 1350–1600 nm. Fig. 14 shows the melt pool images for a single line track on a solid Inconel IN625 sample. As thermal cameras generate an electric signal which is proportional to the temperature of the material, they therefore require calibration or a reference signal for quantitative analysis. The resulting melt pool dimensions and temperature reported in Fig. 14 are therefore approximate and have a degree of error if emissivity is not quantified. Nevertheless, these approximate measurements can be used for build-to-build comparison as a useful measure of process reliability. Arısoy et al. examined an IN625 process using in-situ IR monitoring and compared the results to a simulation using finite element analysis [102]. The model agreed reasonably well with the experimental data, and the thermal modelling allowed for prediction of the thermal gradients within the meltpool and the resulting microstructure formation during solidification. However, it should be noted that there is no reliable way to generalise this data to parts with different geometries or to parts produced using different build conditions, and thus this approach is currently limited to the enhance prediction of part microstructures where matching in-situ thermal data exists.

Bayle et al. combined and compared the two measurement methods, with the dual IR imaging and pyrometry setup shown in demonstrating the ability for highly accurate spatial and temporal measurement of the thermal gradients present in the PBF process [103]. Chivel et al. used a similar dual pyrometer/IR imaging arrangement allowing for accurate measurement of both the thermal distribution and the peak temperature [104], again demonstrating the potential advantages to multiple sensing approaches in a single system.

In contrast to the approaches used in L-PBF processes, in E-PBF processes, it is not possible to mount optics co-axially with the electron beam, and the vacuum atmosphere can allow for vaporised material to condense on optics and the viewing windows within the system. As such, modifications must be made to allow thermal imaging [82,105]. Schwerdtfeger et al. [105] mounted the IR camera inside the build chamber on an E-PBF machine at a 15° angle with respect to the e-beam axis, and placed a ZnSe window in front of the camera for protection, as shown Fig. 15. This demonstrates that IR thermal imaging can be conducted on E-PBF processes when the appropriate modifications are made. Ultimately, as advances are made in thermal measurement, some technologies developed for E-PBF may be suitable for L-PBF and vice versa, and consideration should be given to adapting these or existing techniques where feasible.

3.5. *Commercial systems with in-situ sensing*

To date there are several L-PBF machine Original Equipment

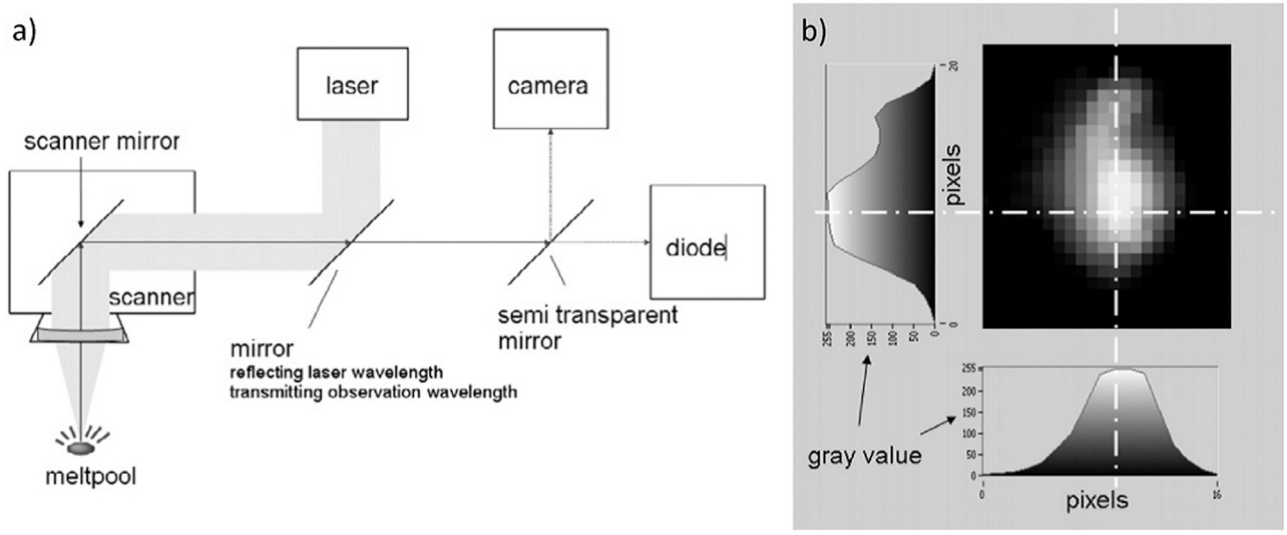

Fig. 12. Schematic of (a) in-line camera and photodiode assembly, and (b) image of the melt pool showing the varying intensity. Reproduced from [40].

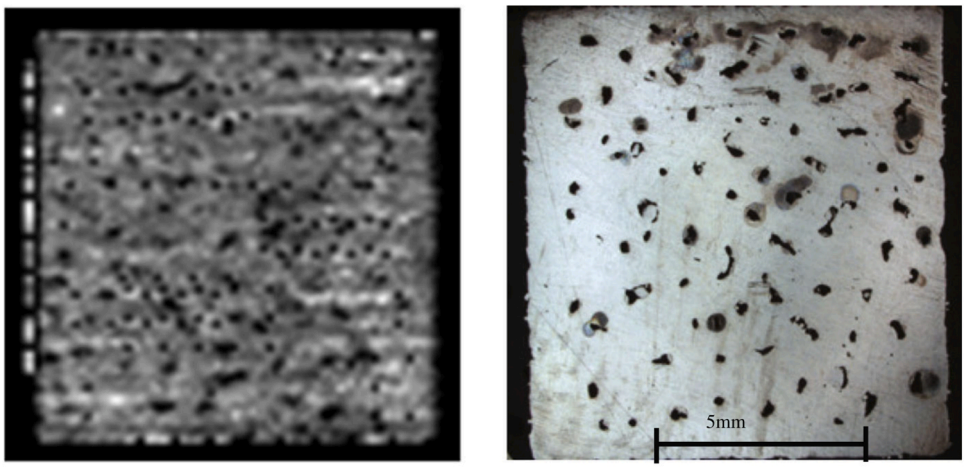

(a) Mapping of the X,Y-plane (b) Microscope image of a X,Y-plane

Fig. 13. Comparison between (a) computed map and (b) microscope image showing pores formed in an AlSi10Mg part. Reproduced from [101].

Manufacturers (OEMs) providing systems equipped with in-situ process monitoring capabilities. The added benefits of integrated process monitoring, such as process fault detection, are especially valuable when the machine is in a production environment or when a new part design or material is being deployed. This is an area of rapid development and what is presented here will no doubt change quickly in the coming years as novel sensing approaches become validated through the current extensive research and development.

Renishaw PLC produce L-PBF systems that are equipped with both laser and melt pool monitoring capabilities. Their system, known as InfiniAM, can provide information on the operational behaviour of the laser, through the LaserView module, while the MeltView module provides insight into the stability and temperature of the melt pool. LaserView measures the intensity of the laser input at rates of up to 2 MHz for every pulse of the laser. This can allow for any deviation or drift in the laser to be easily identified. This relative measurement of laser power can also be combined with system calibration information to monitor the laser performance over long periods of time. The MeltView system uses co-axial photodiode to monitor the emissions generated by the melt pool. Visible plasma emissions in the 300–700 nm wavelength and IR emissions in the 700–1700 nm wavelength ranges are captured using this system. The preparatory Spectral software then converts this data into 2D and 3D representations, in order to give visual feedback to the user [106]. More recently, Renishaw launched their acoustic monitoring system, InfiniAM Sonic. This system is composed of four high frequency acoustic sensors that detect vibrations from different locations on the build platform. By comparing the time at which specific sounds are detected by each of the four microphones, it is possible to estimate the location of the emission. The user is then presented with this data, including the uncertainty in the position, thus aiding users in early potential fault detection [107].

SLM Solutions GmbH, providers of a range of L-PBF systems, also provide laser and melt pool monitoring systems. Their Laser Power Monitoring (LPM) is an on-axis system that provides feedback on the actual and target emitted laser power. Time based recordings are taken of the actual laser power, allowing any slow but constant deviations in the laser performance to be detected. The associated software immediately provides data relating to the actual, target and the percentage deviation between the two [108]. SLM solutions on axis Melt Pool Monitoring (MPM) system records the thermal radiation emitted from the melt pool during the production process. The melt pool thermal radiation, recorded at a rate of 100 kHz, is measured by a dual photodiode array. This data is synchronised with the laser x/y positions and is displayed instantly within the software. This system can be used to optimise the process parameters of individual components [109].

Velo 3D Inc. offers an in-situ process monitoring capabilities through its Assure system. The Assure system uses multiple sensor to predict the bulk properties of components produced on their L-PBF machines. Off-axis sensors are utilised to map the powder layer, allowing for protrusions through the powder to be detected. Similar to other in-situ monitoring systems, Assure used on-axis sensors to monitor the melt pool emissions generated during the build process. Unlike some monitoring systems, however, Assure provides a method of assessing the health of the L-PBF machine prior to commencing a build. The system is capable of monitoring the optical set up, sensors, consumables, and powder bed quality prior to and during the build, and displays the data directly on a user dashboard [110].

Concept Laser GmbH, a GE Additive company, have a suite of in-situ process monitoring capabilities. QM coating module uses a camera to monitor the powder bed after recoating. The system can detect whether sufficient powder has been deployed or not, the system can then adjust the powder dose to suit. QM Melt pool 3D is a co-axial system that monitors melt pool emissions. This system can determine the size and intensity of the melt pool created during the process. A 3D visualisation tool is then used to inform the operator of the intensity of the melt pool emissions [111].

Aconity3D GmbH manufacture systems which optionally include on-axis high-speed camera and pyrometry systems for melt pool monitoring in each of their machines [112]. Their camera system uses a high-speed CMOS, and a secondary low power laser for illumination of the melt pool area. Their pyrometry system incorporates 2 high-speed pyrometers, operating at NIR with a repetition rate of 100 kHz. These monitoring systems are controlled by the same Aconity Studio software that controls the L-PBF system to which they are attached. This software allows for real-time process monitoring and allows the pyrometry unit to produce pyrometric tomography scans by creating layer-by-layer emission maps. These systems scans can then be used for the optimisation of process parameters for part production.

It is noted that the Panda™ L-PBF system from Open Additive LLC. can be configured with the optional AMSENSE® data collection and analysis platform [113]. Available process sensing modules include real-time photo and video imaging of the build area as standard with optional high-resolution recoating imaging, NIR tomography and splatter tracking are available. These modules are also available as stand-alone units for integration in other manufacturer's L-PBF systems.

Aside from machine OEM's, companies such as Sigma Labs supply in-

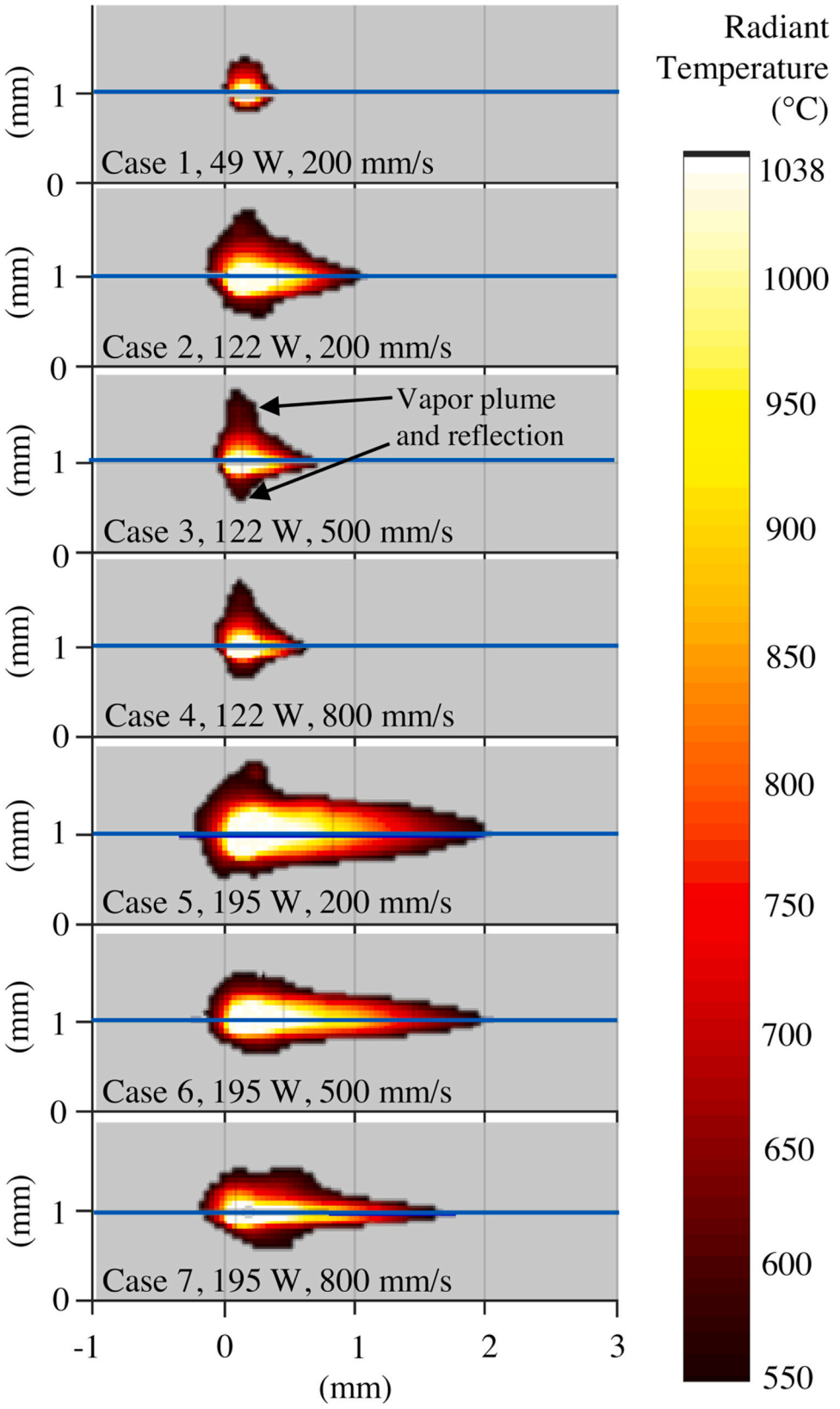

Fig. 14. IR images of the resultant melt pool for seven sets of process parameters using Inconel IN 625 as the feedstock material. Reproduced from [99].

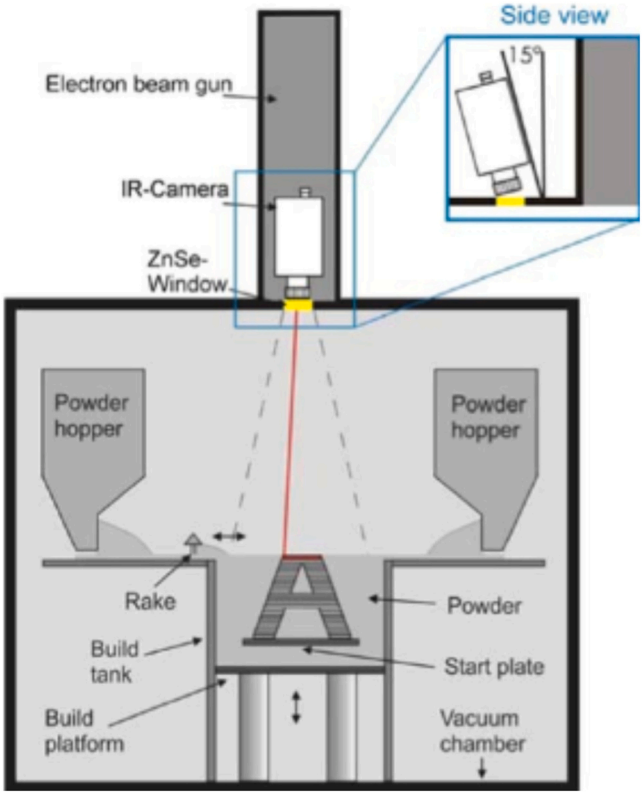

Fig. 15. Process monitoring arrangement in an E-PBF machine [105].

situ process monitoring systems that can be retrofitted to L-PBF machines. Sigma Labs technology includes both on-axis and off-axis sensors to monitor the build process. Proprietary quality metrics can provide the user with an indication of the quality of the build [114]. A comparison of commercially available monitoring system is shown in Table 2. While a broad range of approaches from commercial systems is available, the systems listed in Table 2 are in no way exhaustive and many other PBF suppliers and third-party process monitoring systems are available.

4. Real-time process control

4.1. Requirements for real-time control

Real-time process control describes the use of in-situ monitoring of process signals and part properties to provide feedback, which is used to modify the build parameters during the process in a closed loop. PBF methods are sensitive processes, with a large number of process parameters and possible defects which are influenced by these parameters. The large number of interacting controllable and fixed parameters creates a highly dynamic and complex melt pool environment; encompassing the varied absorption of the beam by the powder and melt pool, melting and resolidification, wetting behaviour, heat conduction, capillary effects, gravity, etc. [115].

Despite the sophistication and numerical control involved in AM, it is often operated as an open-loop process, with process parameters being manually tuned by users based on post-process characterisation and analysis [116,117]. As an open-loop process, corrective actions can only be taken post-process, which may limit the achievable part quality and be wasteful of time, materials, and energy [115,118]. Real-time process control allows for corrective actions to be taken during the process, maximising build quality, consistency, and reproducibility, and eliminating this waste [119]. Many local geometric features, such as sharp corners, are difficult to produce using the fixed processing parameters that are optimised for the bulk of the build [120]. Real-time process control could allow continuous adjustment of the process parameters to allow the desired melt pool and heat transport behaviour for local geometries through-out a part.

Table 2
Examples of commercially available in-situ monitoring systems.

Supplier	Module Name	On/Off Axis	Area Measured	Measurement Technique
Renishaw	MeltView	On	Melt pool	Thermal
	LaserView	On	Laser spot	Optical
	Sonic	–	Build platform	Acoustic
SLM	LaserPowerMonitoring	On	Laser spot	Optical
	Melt Pool Monitoring	On	Melt pool	Thermal
Velo	Assure	On	Laser spot	Optical
		On	Melt pool	Thermal
		Off	Powder bed	Optical
Concept Laser	QM fibre power	On	Laser spot	Optical
	QM Coating	Off	Powder bed	Optical
	QM melt spool 3D	On	Melt pool	Thermal
Sigma Labs	Printrite3D sensorpak	On	Melt pool	Thermal
	Printrite3D inspect	Multiple	Melt pool	Thermal
	Printrite3D contour	Off	Part Geometry	Optical
Aconity3D	Process Monitoring High-Speed Camera	On	Melt pool	Thermal
	Process Monitoring Pyrometer	On	Melt pool	Thermal
Open Additive	AMESENSE Recoating Imaging	–	Build Platform	Optical
	AMSENSE NIR Tomography	–	Build Platform	Optical
	AMSENSE Splatter Tracking	–	Build Platform	Optical

A report by Mani et al., on the needs for real-time process control broke down the PBF process into the relation of its process parameters, signatures, and product qualities, as shown in Fig. 16 [118]. The input process parameters are divided into controllable, those that could be continuously modified during the processing such as laser power, and predefined, those that are fixed from the beginning of the build such as powder size and distribution. The process signatures - the characteristics of the process which may be monitored during the process - are divided into those which are directly observable, such as melt pool shape and temperature, and those which can be derived from modelling, such as residual stresses. Finally the product qualities, the properties of the parts being built, can be divided into geometric, mechanical, and physical properties. Real-time control requires that the correlations indicated in Fig. 16 be identified, developing comprehensive process maps, so that in-process sensing of the process signatures can be used for real-time control of the processing parameters, to achieve the desired product qualities.

It is worth noting, that the process signature to product quality correlation has been more extensively examined than other correlations. More research is needed to fully explore the correlations between process parameters and process signals, and between process parameters

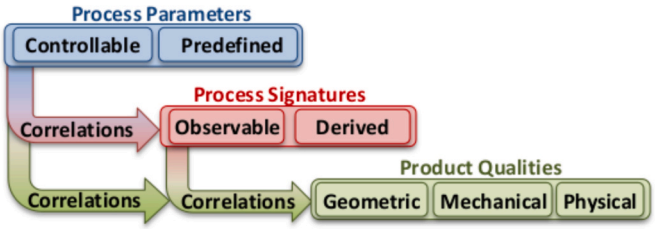

Fig. 16. The relations between process parameters, process signatures, and product qualities in the PBF process.
Reproduced from [118].

and product quality. If this holistic approach is taken to explore these causal relationships, this will allow the development of more robust models, and enhance model transferability from process-to-process, especially where machine learning approaches are used.

Real-time process control requires robust in-process monitoring tools. These tools must be:

1. Fast and responsive to deliver real-time feedback in timeframes that the machine can take corrective action.
2. Compact and affordable, to allow them to be mounted and operated in-situ on commercial AM systems.

Hardware and software architecture is needed for communication of the monitoring data, interpretation of this data in-terms of the correlations and desired properties, and adjustment of the controllable processing parameters during the build [33].

4.2. Current state-of-the-art

Real-time process control for PBF based AM methods is still in its development stages [116,121], with much of the research mainly focused on investigation of the real-time monitoring processes, and determination of the correlations and process maps necessary for real-time process control [122–126].

Some researchers have proposed or simulated designs for real-time process control systems for PBF. Vlasea et al. describe the development of a PBF test bed for implementing and assessing process monitoring methods and real-time process control algorithms [121]. The authors present an organisational structure for the measurement and process control strategy, see Fig. 17.

The strategy includes pre-processing, in-situ defect or fault detection, in-situ continuous feedback control, and signature-derived control. Pre-processing is a digital strategy where part models are compositional and topologically optimised before building and thus can be a significant step towards the final optimised process [128–131].

In-situ defect or fault detection is a simple real-time process control strategy, where the controller responds to defects or faults by triggering defined actions, interrupting the normal build routine to take a discrete corrective action, or halting the build to minimise waste and risk to the equipment. This strategy can be applied independently, or in complementary combination with continuous feedback control. Errors like recoater collisions, contaminants, poor powder spread, or powder exhaustion can be managed with this strategy. While there has been research into defect detection by in-situ monitoring [132–134], more work is needed to develop these into process control systems [121].

In-situ continuous feedback control allows for the controllable process parameters to be continuously adjusted based on feedback from the monitored process signatures. For PBF, the focus is typically on monitoring of the melt pool and plasma plume [95,120,132,135,136]. Kruth et al. outline a method of continuous feedback control for PBF, using CMOS camera and photodiode monitoring of the melt pool [120]. The photodiode captures the melt pool radiation, allowing estimation of the melt pool area, and the CMOS camera captures a 2D image allowing determination of the melt pool geometry. In-situ continuous feedback control was implemented to adjust the laser power in real-time to maintain a more stable melt pool area throughout the build. The authors built benchmark parts containing difficult-to-produce overhang structures with and without feedback control, and found improved results. This illustrates how real-time control can improve part quality.

The final control strategy described by Vlasea et al. is signature-derived control [127]. In this strategy, estimations derived from modelling or simulation algorithms which use monitoring data as inputs are used to infer quantities that can't be directly measured in-process. This requires process maps which can relate immeasurable quantities to those which can be measured. Research for process control of PBF is still primarily in the stage of development of these process maps [115,123]. However, such control approaches have been implemented for some non-PBF-based laser manufacturing methods such as laser cladding. For example, Devesse et al. designed a model-based controller with temperature feedback for laser cladding [137].

4.3. Machine learning-based process control

Machine Learning (ML) describes a class of artificial intelligence algorithms that continue to learn and improve with further data. There are a number of bio-inspired approaches and algorithms relevant in manufacturing contexts [138,139]. Biological systems such as neural or developmental systems have been noted for their suitability for process

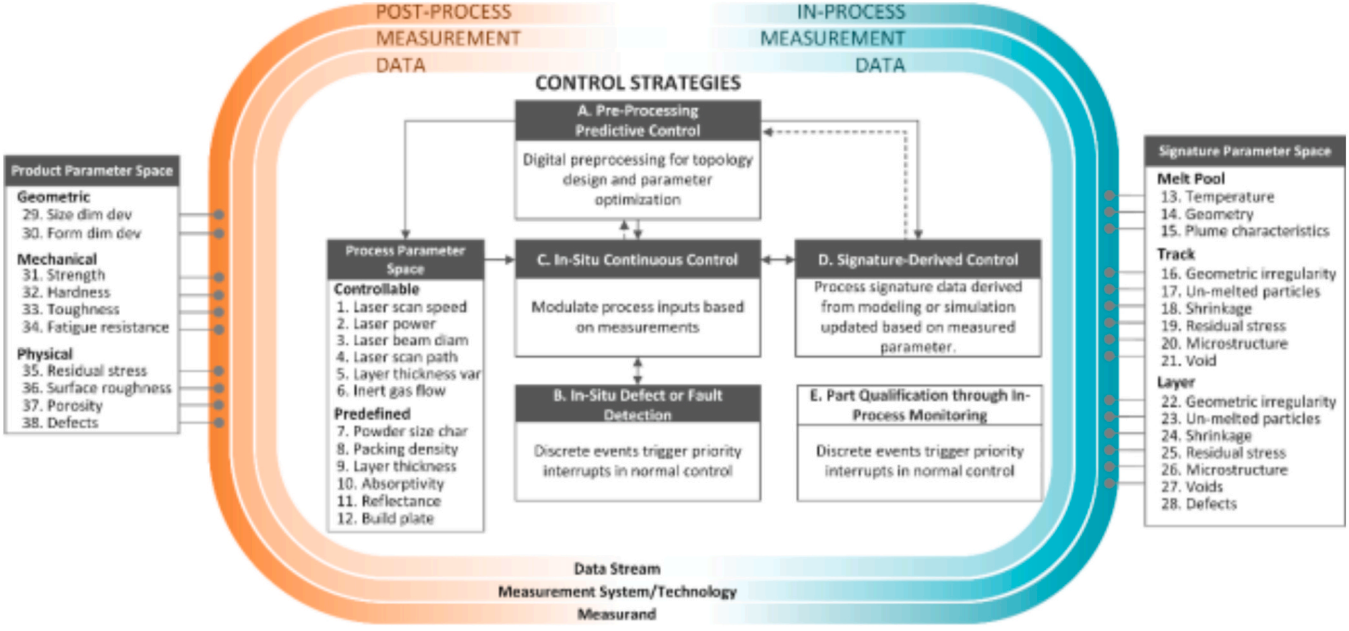

Fig. 17. Measurement organisational structure for possible PBF process control. Developed by Vlasea et al. [127]

modelling, monitoring and real-time control. Though suitable, significant differences between bio-inspired and true biologically intelligent approaches, such as the requirement for bio-inspired artificial intelligence lacking creativity and must be to be optimised for highly specific tasks [26,139]. ML has been widely applied across a range of AM processes and has been extensively reviewed elsewhere, [140,141]. As detailed in prior sections, the AM process has a large number of interacting process parameters, measurable and immeasurable process characteristics, and final part properties. The use of ML has allowed the prediction of part properties such as compressive strength, tensile strength or printability in processes such as Fused Filament Fabrication (FFF) [142], Binder Jetting [143] and Vat Photopolymerisation [144]. ML has also been applied to PBF processes for the estimation of process variables such as build time [143] or part properties such as porosity [145]. The approach to use process parameters such as part height, laser energy density or scan strategy can be useful information for ML algorithms, allowing correlation to final part property.

Though more complex, the use of ML towards process monitoring via in-situ sensing presents an attractive prospect for potential investigation. The real-time nature, and often high sampling rate, of the sensors used in AM, are well suited for ML, and has become an increasingly active area of research. One example from Delli et al. implemented a ML approach to process control in an FFF process utilising real-time data from in-situ optical imaging [24]. Though there were drawbacks identified, including increased build time, significant benefits were realised such as the ability to recognise process issues such as feedstock exhaustion, or the formation of geometric defects.

ML algorithms require large amounts of input data, with models continuing to learn and improve with further data. The potentially high volume of data from PBF, from input part models to in-situ process monitoring data to post-process part property data, make the process highly suitable for a ML approach. However it should be noted that processing this data in real time can require significant computational power and thus there may be a need to filter the available input data for these ML algorithms to be successfully deployed for real-time applications. Furthermore, the volume and complexity of process factors and responses in a PBF process may result in a large volume of coincidental correlations, making the identification of causal relationships difficult using ML solely. Despite this, ML may be useful in identifying the correlations and developing the process maps which are needed for real-time process control, especially when conventional analytical approaches are insufficient.

Some researchers have applied ML approaches to PBF, to improve selection of parameters, simulation and modelling of the process, and in some works to develop towards real-time process control. For example, the use of in-situ imaging and ML has allowed for the prediction of part properties such as geometric defects [146] and porosity and balling [147], or identification of process issues such as recoating errors [148] and overmelting [51,149].

Silbernagel et al. applied ML to parameter optimisation for PBF [150]. The authors collected optical images during production of pure copper parts in a laser PBF machine for manual parameter optimisation. The images were segmented into image patches which were clustered using a ML algorithm. The clusters could then be manually evaluated for whether they represented a good quality result, and assigned a score. The algorithm could then be applied as a parameter optimisation tool, and was found to identify the optimal parameters that would be chosen by manual optimisation. The authors note that this approach could be developed to allow in-situ assessment and parameter control.

Özel et al. developed a ML algorithm for areal surface measurements of nickel alloy 615 [151]. Though the algorithm was trained using data that was gathered from post-build focus variation microscopy, it demonstrated the ability to predict areal surface morphology parameters such as arithmetic mean height, skewness and kurtosis in the xy (top, as built) and to a lesser extent yz (side, as built) planes. If coupled with in-situ surface monitoring, the ML algorithm would be well suited towards defect detection of though measurement of variation of part surfaces.

Scime et al. applied an unsupervised ML algorithm to anomaly detection via camera monitoring [117]. Raw images were captured by the stock powder-bed imaging camera on an EOS M290 machine, and broken down into patches which could be manually determined to contain or not contain a given powder-spreading related anomaly. A database of image patches was developed and used to train the ML algorithm. The trained algorithm could successfully identify and classify anomalies using the stock illumination and imaging equipment on the machine. It was applied as a post-build analysis tool, however the authors note that the algorithm could be developed for real-time process control.

Gobert et al. implemented a supervised ML algorithm to detect defects by correlating in-situ camera monitoring with post-build computed tomography (CT) [152]. High resolution CT scanning is a useful technique for detecting defects and porosity, and evaluating finished parts, however it can only be performed post-build. By training a ML algorithm with anomaly data from CT scans, defects may be detected during the build via in-situ monitoring. In this work a DSLR camera was used to monitor the build layer by layer, generating an image stack for the build. The location of defects within finished parts were identified using an automated anomaly detection methodology for post-build high--resolution 3D CT scanning. The detected anomalies were related to the image stacks, and used to train the ML algorithm. The authors report that the trained algorithm had in-situ defect detection accuracies of greater than 80%, which may be improved with further data.

Wasmer et al. applied ML to in-situ monitoring of acoustic emissions in PBF [153]. The authors used a fibre Bragg grating with a tuneable laser and photodiode as an acoustic sensor (shown in Fig. 18) for in-situ monitoring during AM manufacturing of stainless steel parts using a Concept M2 LPBF machine with a range of scanning velocities. The workpieces produced were classified as either poor, medium, or high quality, and a ML algorithm trained to identify the quality from the acoustic emission data. Once trained, the algorithm could identify the quality with a confidence level of 74–82%. Again, ML algorithms improve with increasing amounts of data, as such this initial result is promising and may be improved with further optimisation.

The above studies illustrate the usefulness of ML algorithms. Due to the complexity of PBF and the high volumes of data, ML has a high suitability to improving AM methods and aiding in the implementation of real-time process control. However, more work is needed to developed full closed-loop systems.

5. Conclusions and outlook

Process sensing and monitoring is finding slow but increasing acceptance in L-PBF processes. Thermal, optical, acoustic and other signals are present in the process, and through the monitoring of these signals, it has been possible to gain significant understanding of the physical mechanisms occurring during the build process. While each individual sensing approach allows monitoring of specific processes or part qualities during the build, considerations such as resolutions, cost and integration requirements must be balanced and tailored for each

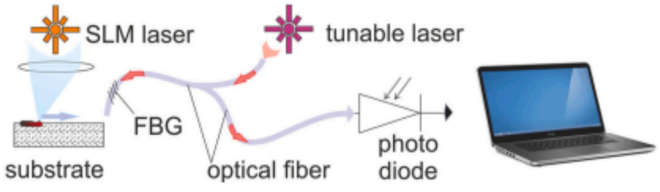

Fig. 18. Fibre Bragg grating acoustic emission monitoring system for use with LPBF.
Reproduced from [153].

process as needed especially when employed in production environments. Despite significant progress made in gathering data from the build process, there are still large roadblocks towards applying these sensing approaches real-time control of a PBF process, such as:

- Integration of multiple process sensors to allow for deeper understanding of the PBF process and the various properties of relevance to a particular build.
- Large-scale data processing and correlation of multiple sensor signals in real-time.
- The development of machine learning algorithms capable of anomaly detection and close-loop control, allowing for reduced operator input to the build process.

While these are all areas currently under investigation, there remains significant scope for the development of new process sensing approaches or sensor integration strategies. As this field matures further, we will no doubt see combination of sensing approaches being developed and further advances towards closed-loop smart control being applied. Each development shows promise to increase reliability while reducing costs for PBF processes, and ultimately allowing greater acceptance of PBF in industry, thus unlocking the full potential of intelligent and sustainable manufacturing technologies such as AM.

Conflicts of interest

The authors declare no conflicts of interest.

Acknowledgements

This publication has emanated from research supported by Science Foundation Ireland (SFI) under Grant Number 16/RC/3872 and is co-funded under the European Regional Development Fund and by I-Form industry partners, and from the European Union's Horizon 2020 Research and Innovation Programme under grant agreement No. 862000.

References

[1] Standard Terminology for Additive Manufacturing – General Principles – Terminology, ISO/ASTM52900-15, ASTM International, West Conshohocken, PA, 2015.
[2] I. Gibson, D.W. Rosen, B. Stucker, Additive Manufacturing Technologies: Rapid Prototyping to Direct Digital Manufacturing, Springer US, Boston, MA, 2010, pp. 1–459.
[3] S.H. Khajavi, J. Partanen, J. Holmström, Additive manufacturing in the spare parts supply chain, Comput. Ind. 65 (1) (2014) 50–63.
[4] G.X. Gu, I. Su, S. Sharma, J.L. Voros, Z. Qin, M.J. Buehler, Three-dimensional-printing of bio-inspired composites, J. Biomech. Eng. 138 (2) (2016).
[5] S. Dietrich, M. Wunderer, A. Huissel, M.F. Zaeh, A new approach for a flexible powder production for additive manufacturing, Procedia Manuf. 6 (2016) 88–95.
[6] L.E. Murr, S.M. Gaytan, D.A. Ramirez, E. Martinez, J. Hernandez, K.N. Amato, P. W. Shindo, F.R. Medina, R.B. Wicker, Metal fabrication by additive manufacturing using laser and electron beam melting technologies, J. Mater. Sci. Technol. 28 (2012) 1–14.
[7] E. Louvis, P. Fox, C.J. Sutcliffe, Selective laser melting of aluminium components, J. Mater. Process Technol. 211 (2) (2011) 275–284.
[8] E. Malekipour, H. El-Mounayri, Common defects and contributing parameters in powder bed fusion AM process and their classification for online monitoring and control: a review, Int. J. Adv. Manuf. Technol. 95 (1–4) (2018 27) 527–550.
[9] S. Hällgren, L. Pejryd, J. Ekengren, 3D data export for additive manufacturing-improving geometric accuracy, Procedia CIRP 50 (2016) 518–523.
[10] Z. Huang, J.Y. Dantan, A. Etienne, M. Rivette, N. Bonnet, Geometrical deviation identification and prediction method for additive manufacturing, Rapid Prototyp. J. 24 (9) (2018) 1524–1538.
[11] C. Douellou, X. Balandraud, E. Duc, Assessment of geometrical defects caused by thermal distortions in laser-beam-melting additive manufacturing: a simulation approach, Rapid Prototyp. J. 25 (5) (2019 10) 939–950.
[12] C. Li, Z.Y. Liu, X.Y. Fang, Y.B. Guo, Residual stress in metal additive manufacturing, Procedia CIRP 71 (2018) 348–353.
[13] K. Wegener, A.B. Spierings, M. Schmid, Additive manufacturing on the way to industrialization, in: Proceedings of the International Conference on Competitive Manufacturing COMA'16 Proc, 2016. pp. 11–22.
[14] M. Tang, P.C. Pistorius, Oxides, porosity and fatigue performance of AlSi10Mg parts produced by selective laser melting, Int. J. Fatigue 94 (2017) 192–201.
[15] R. Esmaeilizadeh, A. Keshavarzkermani, U. Ali, B. Behravesh, A. Bonakdar, H. Jahed, et al., On the effect of laser powder-bed fusion process parameters on quasi-static and fatigue behaviour of Hastelloy X: a microstructure/defect interaction study, Addit. Manuf. 38 (2021), 101805.
[16] R. Shrestha, J. Simsiriwong, N. Shamsaei, Fatigue behavior of additive manufactured 316L stainless steel under axial versus rotating-bending loading: synergistic effects of stress gradient, surface roughness, and volumetric defects, Int. J. Fatigue 144 (2021), 106063.
[17] W. Schneller, M. Leitner, S. Pomberger, F. Grün, S. Leuders, T. Pfeifer, et al., Fatigue strength assessment of additively manufactured metallic structures considering bulk and surface layer characteristics, Addit. Manuf. 40 (2021), 101930.
[18] G.W. Zeng, M.C. Monu, C. Lupton, B. Lin, J. Tong, Towards a fundamental understanding of the effects of surface conditions on fatigue resistance for safety-critical AM applications, Int. J. Fatigue 136 (February) (2020), 105585.
[19] D. Gu, Y. Shen, Balling phenomena in direct laser sintering of stainless steel powder: metallurgical mechanisms and control methods, Mater. Des. 30 (8) (2009) 2903–2910.
[20] J.P. Kruth, P. Mercelis, J. Van Vaerenbergh, L. Froyen, M. Rombouts, Binding mechanisms in selective laser sintering and selective laser melting, Rapid Prototyp. J. 11 (1) (2005) 26–36.
[21] R. Li, J. Liu, Y. Shi, L. Wang, W. Jiang, Balling behavior of stainless steel and nickel powder during selective laser melting process, Int. J. Adv. Manuf. Technol. 59 (9–12) (2012) 1025–1035.
[22] P. Edwards, A. O'Conner, M. Ramulu, Electron beam additive manufacturing of titanium components: properties and performance, J. Manuf. Sci. Eng. Trans. ASME 135 (6) (2013), 061016.
[23] G. Kasperovich, J. Haubrich, J. Gussone, G. Requena, Correlation between porosity and processing parameters in TiAl6V4 produced by selective laser melting, Mater. Des. 105 (2016) 160–170.
[24] U. Delli, S. Chang, Automated process monitoring in 3D printing using supervised machine learning, Procedia Manuf. 26 (2018) 865–870.
[25] J.K. Stroble, R.B. Stone, S.E. Watkins, An overview of biomimetic sensor technology, Sens. Rev. 29 (2) (2009) 112–119.
[26] G. Byrne, D. Dimitrov, L. Monostori, R. Teti, F. van Houten, R. Wertheim, Biologicalisation: biological transformation in manufacturing, CIRP J. Manuf. Sci. Technol. 21 (2018) 1–32.
[27] H. Rieder, A. Dillhöfer, M. Spies, J. Bamberg, T. Hess, Online monitoring of additive manufacturing processes using ultrasound, in: Proceedings of the 11th European Conference on Non-Destructive Testing (Ecndt), 2014, 1. pp. 2194–201.
[28] H. Rieder, M. Spies, J. Bamberg, B. Henkel, On- and offline ultrasonic characterization of components built by SLM additive manufacturing, in: Proceedings of the AIP Conference, 2016. p. 130002.
[29] R.J. Smith, M. Hirsch, R. Patel, W. Li, A.T. Clare, S.D. Sharples, Spatially resolved acoustic spectroscopy for selective laser melting, J. Mater. Process. Technol. 236 (2016) 93–102.
[30] S.A. Shevchik, C. Kenel, C. Leinenbach, K. Wasmer, Acoustic emission for in situ quality monitoring in additive manufacturing using spectral convolutional neural networks, Addit. Manuf. 21 (2018) 598–604.
[31] T. Craeghs, S. Clijsters, E. Yasa, J.-P. Kruth, Online quality control of selective laser melting, in: Proceedings of the 22nd Annual International Solid Freeform Fabrication Symposium - An Additive Manufacturing Conference, SFF 2011, 2011. pp. 212–26.
[32] I. Yadroitsev, P. Krakhmalev, I. Yadroitsava, Selective laser melting of Ti6Al4V alloy for biomedical applications: temperature monitoring and microstructural evolution, J. Alloy. Compd. 583 (2014) 404–409.
[33] A.J. Dunbar, A.R. Nassar, E.W. Reutzel, J.J. Blecher, A real-time communication architecture for metal powder bed fusion additive manufacturing, in: Proceedings of the 27th Annual International Solid Freeform Fabrication Symposium, 2016. pp. 67–80.
[34] G. Zenzinger, J. Bamberg, A. Ladewig, T. Hess, B. Henkel, W. Satzger, Process monitoring of additive manufacturing by using optical tomography, in: Proceedings of the AIP Conference, 2015. pp. 164–70.
[35] G. Mohr, S.J. Altenburg, A. Ulbricht, P. Heinrich, D. Baum, C. Maierhofer, et al., In-situ defect detection in laser powder bed fusion by using thermography and optical tomography—comparison to computed tomography, Metals 10 (1) (2020).
[36] A. du Plessis, I. Yadroitsava, I. Yadroitsev, Effects of defects on mechanical properties in metal additive manufacturing: a review focusing on X-ray tomography insights, Mater. Des. 187 (2020), 108385.
[37] A. Du Plessis, I. Yadroitsev, I. Yadroitsava, S.G. Le Roux, X-Ray microcomputed tomography in additive manufacturing: a review of the current technology and applications, 3D Print. Addit. Manuf. 5 (3) (2018) 227–247.
[38] J.A. Kanko, A.P. Sibley, J.M. Fraser, In situ morphology-based defect detection of selective laser melting through inline coherent imaging, J. Mater. Process Technol. 231 (2016) 488–500.
[39] V. Mahato, M. Ahmed, D. Brabazon, P. Cunningham, An evaluation of classification methods for 3D printing time-series data, in: Proceedings of the 21st International Federation of Automation Control (IFAC) World Congress, 2020.
[40] S. Berumen, F. Bechmann, S. Lindner, J.-P. Kruth, T. Craeghs, Quality control of laser- and powder bed-based Additive Manufacturing (AM) technologies, Phys. Procedia 5 (2010) 617–622.

[41] T. Segreto, A. Bottillo, R. Teti, Advanced ultrasonic non-destructive evaluation for metrological analysis and quality assessment of impact damaged non-crimp fabric composites, Procedia CIRP (2016) 1055–1060.

[42] N.P. Aleshin, V.V. Murashov, N.A. Shchipakov, I.S. Krasnov, D.S. Lozhkova, Experimental research into possibilities and peculiarities of ultrasonic testing of additive manufactured parts, Russ. J. Nondestruct. Test. 52 (12) (2016) 685–690.

[43] A.A. Popovich, D.V. Masaylo, V.S. Sufiiarov, E.V. Borisov, I.A. Polozov, V. A. Bychenok, I.Y. Kinzhagulov, I.V. Berkutov, D.S. Ashikhin, A.V. Il'inskii, A laser ultrasonic technique for studying the properties of products manufactured by additive technologies, Russ. J. Nondestruct. Test. 52 (6) (2016) 303–309.

[44] S. Everton, P. Dickens, C. Tuck, B. Dutton, Using laser ultrasound to detect subsurface defects in metal laser powder bed fusion components, JOM 70 (3) (2018) 378–383.

[45] D. Ye, G.S. Hong, Y. Zhang, K. Zhu, J.Y.H. Fuh, Defect detection in selective laser melting technology by acoustic signals with deep belief networks, Int. J. Adv. Manuf. Technol. 96 (5–8) (2018) 2791–2801.

[46] D. Buchbinder, H. Schleifenbaum, S. Heidrich, W. Meiners, J. Bültmann, High power Selective Laser Melting (HP SLM) of aluminum parts, Phys. Procedia 12 (2011) 271–278.

[47] B.M. Colosimo, M. Grasso, Spatially weighted PCA for monitoring video image data with application to additive manufacturing, J. Qual. Technol. 50 (4) (2018) 391–417.

[48] B. Zhang, J. Ziegert, F. Farahi, A. Davies, In situ surface topography of laser powder bed fusion using fringe projection, Addit. Manuf. 12 (2016) 100–107.

[49] L. Yang, L. Lo, S. Ding, T. Özel, Monitoring and detection of meltpool and spatter regions in laser powder bed fusion of super alloy Inconel 625, Prog. Addit. Manuf. 5 (4) (2020) 367–378.

[50] L.E. Criales, Y.M. Arısoy, B. Lane, S. Moylan, A. Donmez, T. Özel, Laser powder bed fusion of nickel alloy 625: experimental investigations of effects of process parameters on melt pool size and shape with spatter analysis, Int. J. Mach. Tools Manuf. 121 (September 2016) (2017) 22–36.

[51] L.E. Criales, Y.M. Arısoy, B. Lane, S. Moylan, A. Donmez, T. Özel, Predictive modeling and optimization of multi-track processing for laser powder bed fusion of nickel alloy 625, Addit. Manuf. 13 (2017) 14–36.

[52] G. Repossini, V. Laguzza, M. Grasso, B.M. Colosimo, On the use of spatter signature for in-situ monitoring of Laser Powder Bed Fusion, Addit. Manuf. 16 (2010) (2017) 35–48.

[53] L. Mazzoleni, A.G. Demir, L. Caprio, M. Pacher, B. Previtali, Real-time observation of melt pool in selective laser melting: spatial, temporal, and wavelength resolution criteria, IEEE Trans. Instrum. Meas. 69 (4) (2020) 1179–1190.

[54] H. Baumgartl, J. Tomas, R. Buettner, M. Merkel, A deep learning-based model for defect detection in laser-powder bed fusion using in-situ thermographic monitoring, Prog. Addit. Manuf. 5 (2020) 277–285 (0123456789).

[55] B. Yuan, B. Giera, G. Guss, I. Matthews, S. Mcmains, Semi-supervised convolutional neural networks for in-situ video monitoring of selective laser melting, in: Proceedings of the 2019 IEEE Winter Conference on Applications of Computer Vision (WACV), IEEE, 2019. pp. 744–753.

[56] N.D. Parab, C. Zhao, R. Cunningham, L.I. Escano, K. Fezzaa, W. Everhart, A. D. Rollett, L. Chen, T. Sun, Ultrafast X-ray imaging of laser–metal additive manufacturing processes, J. Synchrotron Radiat. 25 (5) (2018) 1467–1477.

[57] T. Sun, Probing ultrafast dynamics in Laser Powder Bed Fusion using high-speed X-ray imaging: a review of research at the advanced photon source, Jom 72 (3) (2020) 999–1008.

[58] Q. Guo, C. Zhao, M. Qu, L. Xiong, L.I. Escano, S.M.H. Hojjatzadeh, N.D. Parab, K. Fezzaa, W. Everhart, T. Sun, L. Chen, In-situ characterization and quantification of melt pool variation under constant input energy density in laser powder bed fusion additive manufacturing process, Addit. Manuf. 28 (January) (2019) 600–609.

[59] C. Aragón, J.A. Aguilera, Characterization of laser induced plasmas by optical emission spectroscopy: a review of experiments and methods, Spectrochim. Acta - Part B Spectrosc. 63 (9) (2008) 893–916.

[60] Z. Szymański, J. Kurzyna, W. Kalita, The spectroscopy of the plasma plume induced during laser welding of stainless steel and titanium, J. Phys. D: Appl. Phys. 30 (1997) 3153–3162.

[61] H.R. Griem, Principles of Plasma Spectroscopy, Cambridge University Press, 1997.

[62] H.R. Griem, W.L. Barr, Spectral line broadening by plasmas, IEEE Trans. Plasma Sci. 3 (4) (1975) 227, 227-227.

[63] A. Ancona, V. Spagnolo, P.M. Lugarà, M. Ferrara, Optical sensor for real-time monitoring of CO_2 laser welding process, Appl. Opt. 40 (33) (2001) 6019.

[64] P. Sforza, D. De Blasiis, On-line optical monitoring system for arc welding, NDTE Int. 35 (2002) 37–43.

[65] S. Liu, W. Liu, M. Harooni, J. Ma, R. Kovacevic, Real-time monitoring of laser hot-wire cladding of Inconel 625, Opt. Laser Technol. 62 (2014) 124–134.

[66] T. Sibillano, A. Ancona, V. Berardi, E. Schingaro, G. Basile, Mario, P. Lugarà, A study of the shielding gas influence on the laser beam welding of AA5083 aluminium alloys by in-process spectroscopic investigation, Opt. Lasers Eng. 44 (2006) 1039–1051.

[67] A.R. Nassar, R. Akarapu, S.M. Copley, J.A. Todd, Investigations of laser-sustained plasma and its role in laser nitriding of titanium, J. Phys. D: Appl. Phys. 45 (2012), 185401.

[68] L. Song, J. Mazumder, Real time Cr measurement using optical emission spectroscopy during direct metal deposition process, IEEE Sens. J. 12 (2012) 958–964.

[69] A. Kramida, Y. Ralchenko, J. Reader, NIST ASD Team, NIST Atomic Spectra Database (version 5.8) [Internet], National Institute of Standards and Technology, Gaithersburg, MD, 2020.

[70] A.J. Dunbar, A.R. Nassar, Assessment of optical emission analysis for in-process monitoring of powder bed fusion additive manufacturing, Virtual Phys. Prototyp. 13 (2018) 14–19.

[71] C.S. Lough, L.I. Escano, M. Qu, C.C. Smith, R.G. Landers, D.A. Bristow, et al., In-situ optical emission spectroscopy during SLM of 304L stainless steel, in: Proceedings of the 29th Annual International Solid Freeform Fabrication Symposium, 2018. pp. 2192–201.

[72] M. Montazeri, A.R. Nassar, A.J. Dunbar, P. Rao, In-process monitoring of porosity in additive manufacturing using optical emission spectroscopy, IISE Trans. 52 (2020) 500–515.

[73] C.B. Stutzman, A.R. Nassar, E.W. Reutzel, Multi-sensor investigations of optical emissions and their relations to directed energy deposition processes and quality, Addit. Manuf. 21 (January) (2018) 333–339.

[74] C.S. Lough, L.I. Escano, M. Qu, C.C. Smith, R.G. Landers, D.A. Bristow, L. Chen, E. C. Kinzel, In-situ optical emission spectroscopy of selective laser melting, J. Manuf. Process. 53 (February) (2020) 336–341.

[75] A. du Plessis, M. Tshibalanganda, S.G. le Roux, Not all scans are equal: X-ray tomography image quality evaluation, Mater. Today Commun. 22 (September 2019) (2020), 100792.

[76] A. Townsend, L. Pagani, P. Scott, L. Blunt, Areal surface texture data extraction from X-ray computed tomography reconstructions of metal additively manufactured parts, Precis. Eng. 48 (2017) 254–264.

[77] P. Lhuissier, X. Bataillon, C. Maestre, J. Sijobert, E. Cabrol, P. Bertrand, E. Boller, A. Rack, J.J. Blandin, L. Salvo, G. Martin, In situ 3D X-ray microtomography of laser-based powder-bed fusion (L-PBF)—a feasibility study, Addit. Manuf. 34 (December 2019) (2020), 101271.

[78] A. Neef, V. Seyda, D. Herzog, C. Emmelmann, M. Schönleber, M. Kogel-Hollacher, Low coherence interferometry in selective laser melting, Phys. Procedia 56 (C) (2014) 82–89.

[79] N. Senin, A. Thompson, R.K. Leach, Characterisation of the topography of metal additive surface features with different measurement technologies, Meas. Sci. Technol. 28 (9) (2017), 095003.

[80] P.J. DePond, G. Guss, S. Ly, N.P. Calta, D. Deane, S. Khairallah, M.J. Matthews, In situ measurements of layer roughness during laser powder bed fusion additive manufacturing using low coherence scanning interferometry, Mater. Des. 154 (2018) 347–359.

[81] I. Smurov, M. Doubenskaia, Temperature monitoring by optical methods in laser processing, in: Springer Series in Materials Science, Springer, 2013, pp. 375–422.

[82] R.B. Dinwiddie, R.R. Dehoff, P.D. Lloyd, L.E. Lowe, J.B. Ulrich, Thermographic in-situ process monitoring of the electron-beam melting technology used in additive manufacturing, in: Proceedings of the Thermosense: Thermal Infrared Applications XXXV, 2013. p. 87050K.

[83] J. Raplee, A. Plotkowski, M.M. Kirka, R. Dinwiddie, A. Okello, R.R. Dehoff, S. S. Babu, Thermographic microstructure monitoring in electron beam additive manufacturing, Sci. Rep. 7 (March) (2017) 1–16.

[84] E. Rodriguez, J. Mireles, C.A. Terrazas, D. Espalin, M.A. Perez, R.B. Wicker, Approximation of absolute surface temperature measurements of powder bed fusion additive manufacturing technology using in situ infrared thermography, Addit. Manuf. 5 (2015) 31–39.

[85] L. González-Fernández, E. Risueño, R.B. Pérez-Sáez, M.J. Tello, Infrared normal spectral emissivity of Ti-6Al-4V alloy in the 500–1150 K temperature range, J. Alloy. Compd. 541 (2012) 144–149.

[86] G. Teodorescu, P.D. Jones, R.A. Overfelt, B. Guo, Normal emissivity of high-purity nickel at temperatures between 1440 and 1605 K, J. Phys. Chem. Solids 69 (1) (2008) 133–138.

[87] B. Kong, T. Li, Q. Eri, Normal spectral emissivity of GH536 (HastelloyX) in three surface conditions, Appl. Therm. Eng. 113 (2017) 20–26.

[88] J. Zueco, F. Alhama, Inverse estimation of temperature dependent emissivity of solid metals, J. Quant. Spectrosc. Radiat. Transf. 101 (1) (2006) 73–86.

[89] R.J. Williams, A. Piglione, T. Rønneberg, C. Jones, M.S. Pham, C.M. Davies, P. A. Hooper, In situ thermography for laser powder bed fusion: effects of layer temperature on porosity, microstructure and mechanical properties, Addit. Manuf. 30 (2019), 100880.

[90] P.A. Hooper, Melt pool temperature and cooling rates in laser powder bed fusion, Addit. Manuf. 22 (May) (2018) 548–559.

[91] S.A. Khairallah, A.T. Anderson, A. Rubenchik, W.E. King, Laser powder-bed fusion additive manufacturing: physics of complex melt flow and formation mechanisms of pores, spatter, and denudation zones, Acta Mater. 108 (2016) 36–45.

[92] N. Thermometry, Pyrometer- Handbook.

[93] S. Kumar, Selective laser sintering: a qualitative and objective approach, JOM 55 (10) (2003) 43–47.

[94] M. Pavlov, M. Doubenskaia, I. Smurov, Pyrometric analysis of thermal processes in SLM technology, Phys. Procedia 5 (2010) 523–531.

[95] T. Craeghs, F. Bechmann, S. Berumen, J.-P. Kruth, Feedback control of Layerwise Laser Melting using optical sensors, Phys. Procedia 5 (2010) 505–514.

[96] P. Lott, H. Schleifenbaum, W. Meiners, K. Wissenbach, C. Hinke, J. Bültmann, Design of an optical system for the in situ process monitoring of Selective Laser Melting (SLM), Phys. Procedia 12 (2011) 683–690.

[97] T. Craeghs, S. Clijsters, J.P. Kruth, F. Bechmann, M.C. Ebert, Detection of process failures in Layerwise Laser Melting with optical process monitoring, Phys. Procedia 39 (2012) 753–759.

[98] S.K. Everton, M. Hirsch, P.I. Stavroulakis, R.K. Leach, A.T. Clare, Review of in-situ process monitoring and in-situ metrology for metal additive manufacturing, Mater. Des. 95 (2016) 431–445.

[99] J.C. Heigel, B.M. Lane, Measurement of the melt pool length during single scan tracks in a commercial Laser Powder Bed Fusion Process, J. Manuf. Sci. Eng. Trans. ASME 140 (5) (2018) 1–8.

[100] F. Herzog, F. Bechmann, S. Berumen, J.P. Kruth, T. Craeghs, Inventors Method for Producing a Three-Dimensional Component Patent WO 1996008749 A3, 2013.

[101] S. Clijsters, T. Craeghs, S. Buls, K. Kempen, J.-P. Kruth, In situ quality control of the selective laser melting process using a high-speed, real-time melt pool monitoring system, Int. J. Adv. Manuf. Technol. 75 (5–8) (2014) 1089–1101.

[102] Y.M. Arısoy, L.E. Criales, T. Özel, Modeling and simulation of thermal field and solidification in laser powder bed fusion of nickel alloy IN625, Opt. Laser Technol. 109 (June 2018) (2019) 278–292.

[103] Bayle F., Doubenskaia M., Selective laser melting process monitoring with high speed infra-red camera and pyrometer", Proc. SPIE 6985, Fundamentals of Laser Assisted Micro- and Nanotechnologies, 698505 (15 January 2008).

[104] Y. Chivel, I. Smurov, On-line temperature monitoring in selective laser sintering/melting, Phys. Procedia 5 (2010) 515–521.

[105] J. Schwerdtfeger, R.F. Singer, C. Körner, In situ flaw detection by IR-imaging during electron beam melting, Rapid Prototyp. J. 18 (4) (2012) 259–263.

[106] P.L.C Renishaw, InfiniAM Spectral – Energy Input and Melt Pool Emissions Monitoring for AM Systems [Internet]. Report, 2017. p. 1–5.

[107] TCT magazine. Renishaw Launches “first of its kind” Acoustic Process Monitoring Software for Metal 3D Printing Technology, 2019.

[108] S. Solutions, Additive Quality-LPM.

[109] SLM Solutions, Additive Quality- MPM.

[110] Assure, Assure Quality Assurance and Control System, 2019.

[111] ConceptLaser. Achieve the Highest Possible Quality in Series Production Thanks to LaserCUSING ® [Internet] Report, 2015. pp. 1–4.

[112] Aconity GmbH. Equipment - Aconity3d [Internet], 2020. p. ⟨https://aconity3d.com/equipment/⟩.

[113] The Pandatm Metal 3D Printing System, 2021. p. ⟨https://openadditive.com/#panda⟩.

[114] L. Jacquemetton, S. Betts, D. Beckett, PrintRite3D Alerts for Anomaly Detection, 2019.

[115] C. Körner, E. Attar, P. Heinl, Mesoscopic simulation of selective beam melting processes, J. Mater. Process. Technol. 211 (6) (2011) 978–987.

[116] Z. Wang, C.P. Pannier, K. Barton, D.J. Hoelzle, Application of robust monotonically convergent spatial iterative learning control to microscale additive manufacturing, Mechatronics 56 (October) (2018) 157–165.

[117] L. Scime, J. Beuth, Anomaly detection and classification in a laser powder bed additive manufacturing process using a trained computer vision algorithm, Addit. Manuf. 19 (2018) 114–126.

[118] M Mani, BM Lane, MA Donmez, SC Feng, SP Moylan, A review on measurement science needs for real-time control of additive manufacturing metal powder bed fusion processes, Int. J. Prod. Res. 55 (2016) 1400–1418.

[119] M. Mani, S. Feng, B. Lane, A. Donmez, S. Moylan, R. Fesperman, Measurement science needs for real-time control of additive manufacturing powder-bed fusion processes. Additive Manufacturing Handbook: Product Development for the Defense Industry, 2017, pp. 629–676.

[120] J.P. Kruth, P. Mercelis, J. Van Vaerenbergh, Feedback control of selective laser melting, in: Proceedings of the 15th International Symposium on Electromachining, ISEM 2007, 2007. pp. 421–6.

[121] M.L. Vlasea, B. Lane, F. Lopez, S. Mekhontsev, A. Donmez, Development of powder bed fusion additive manufacturing test bed for enhanced real-time process control, in: Proceedings of the 26th Annual International Solid Freeform Fabrication Symposium, 2015, (August). pp. 527–39.

[122] C. Zhao, K. Fezzaa, R.W. Cunningham, H. Wen, F. De Carlo, L. Chen, A.D. Rollett, T. Sun, Real-time monitoring of laser powder bed fusion process using high-speed X-ray imaging and diffraction, Sci. Rep. 7 (1) (2017) 1–11.

[123] A. Hussein, L. Hao, C. Yan, R. Everson, Finite element simulation of the temperature and stress fields in single layers built without-support in selective laser melting, Mater. Des. 52 (2013) 638–647.

[124] T.H.G. Childs, G. Hauser, M. Badrossamay, Selective laser sintering (melting) of stainless and tool steel powders: experiments and modelling, Proc. Inst. Mech. Eng. Part B: J. Eng. Manuf. 219 (2005) 339–357.

[125] R. Li, Y. Shi, J. Liu, H. Yao, W. Zhang, Effects of processing parameters on the temperature field of selective laser melting metal powder, Powder Metall. Met. Ceram. 48 (3–4) (2009) 186–195.

[126] G. Bugeda, M. Cervera, G. Lombera, Numerical prediction of temperature and density distributions in selective laser sintering processes, Rapid Prototyp. J. 5 (1) (1999) 21–26.

[127] M.L. Vlasea, B. Lane, F. Lopez, S. Mekhontsec, A. Donmez, Test bed for enhanced real-time process control, Natl. Inst. Stand. Technol. (2015) 527–539.

[128] C. Emmelmann, P. Sander, J. Kranz, E. Wycisk, Laser additive manufacturing and bionics: redefining lightweight design, Phys. Procedia 12 (PART 1) (2011) 364–368.

[129] L. Yang, O.L.A. Harrysson, D. Cormier, H. West, S. Zhang, H. Gong, et al., Design for additively manufactured lightweight structure: a perspective, in: Proceedings of the 27th Annual International Solid Freeform Fabrication Symposium, 2016. pp. 2165–80.

[130] Y. Xu, D. Zhang, S. Hu, R. Chen, Y. Gu, X. Kong, J. Tao, Y. Jiang, Mechanical properties tailoring of topology optimized and selective laser melting fabricated Ti6Al4V lattice structure, J. Mech. Behav. Biomed. Mater. 99 (April) (2019) 225–239.

[131] N. Chantarapanich, A. Laohaprapanon, S. Wisutmethangoon, P. Jiamwatthanachai, P. Chalermkarnnon, S. Sucharitpwatskul, P. Puttawibul, K. Sitthiseripratip, Fabrication of three-dimensional honeycomb structure for aeronautical applications using selective laser melting: a preliminary investigation, Rapid Prototyp. J. 20 (6) (2014) 551–558.

[132] T. Craeghs, S. Clijsters, E. Yasa, J.-P. Kruth, Online quality control of selective laser melting, in: Proceedings of the Solid Freeform Fabrication Symposium, 2011. pp. 212–226.

[133] H. Krauss, C. Eschey, M. Zaeh, Thermography for monitoring the Selective Laser Melting Process, in: Proceedings of the Solid Freeform Fabrication Symposium, 2012. pp. 999–1014.

[134] M. Islam, T. Purtonen, H. Piili, A. Salminen, O. Nyrhilä, Temperature profile and imaging analysis of laser additive manufacturing of stainless steel, Phys. Procedia 41 (2013) 835–842.

[135] S. Berumen, F. Bechmann, S. Lindner, J.-P. Kruth, T. Craeghs, Quality control of laser- and powder bed-based Additive Manufacturing (AM) technologies, Phys. Procedia 5 (2010) 617–622.

[136] K.A. Mumtaz, N. Hopkinson, Selective Laser Melting of thin wall parts using pulse shaping, J. Mater. Process. Technol. 210 (2) (2010) 279–287.

[137] W. Devesse, D. De Baere, P. Guillaume, Design of a model-based controller with temperature feedback for laser cladding, Phys. Procedia 56 (C) (2014) 211–219.

[138] L. Monostori, A. Markus, H. Van Brussel, E. Westkämpfer, Machine learning approaches to manufacturing, CIRP Ann. - Manuf. Technol. 45 (2) (1996) 675–712.

[139] D. Floreano, C. Mattiussi, Bio-Inspired Artificial Intelligence: Theories, Methods, and Technologies, MIT Press, Cambridge, MA, 2008.

[140] L. Meng, B. McWilliams, W. Jarosinski, H.-Y. Park, Y.-G. Jung, J. Lee, J. Zhang, Machine learning in additive manufacturing: a review, JOM 72 (6) (2020) 2363–2377.

[141] G.D. Goh, S.L. Sing, W.Y. Yeong, A review on machine learning in 3D printing: applications, potential, and challenges, Artif. Intell. Rev. 54 (1) (2021 16) 63–94.

[142] Ö. Bayraktar, G. Uzun, R. Çakiroğlu, A. Guldas, Experimental study on the 3D-printed plastic parts and predicting the mechanical properties using artificial neural networks, Polym. Adv. Technol. 28 (8) (2017) 1044–1051.

[143] M. Asadi-Eydivand, M. Solati-Hashjin, A. Fathi, M. Padashi, Abu, N.A. Osman, Optimal design of a 3D-printed scaffold using intelligent evolutionary algorithms, Appl. Soft Comput. J. 39 (2016 1) 36–47.

[144] H. He, Y. Yang, Y. Pan, Machine learning for continuous liquid interface production: printing speed modelling, J. Manuf. Syst. 50 (2019) 236–246.

[145] R. Snell, S. Tammas-Williams, L. Chechik, A. Lyle, E. Hernández-Nava, C. Boig, G. Panoutsos, I. Todd, Methods for rapid pore classification in metal additive manufacturing, JOM 72 (1) (2020) 101–109.

[146] F. Caiazzo, A. Caggiano, Laser direct metal deposition of 2024 Al alloy: trace geometry prediction via machine learning, Materials 11 (3) (2018) 444.

[147] L. Scime, J. Beuth, Using machine learning to identify in-situ melt pool signatures indicative of flaw formation in a laser powder bed fusion additive manufacturing process, Addit. Manuf. 25 (2019) 151–165.

[148] F. Caltanissetta, M. Grasso, S. Petrò, B.M. Colosimo, Characterization of in-situ measurements based on layerwise imaging in laser powder bed fusion, Addit. Manuf. 24 (2018) 183–199.

[149] Y. Zhang, G.S. Hong, D. Ye, K. Zhu, J.Y.H. Fuh, Extraction and evaluation of melt pool, plume and spatter information for powder-bed fusion AM process monitoring, Mater. Des. 156 (2018) 458–469.

[150] C. Silbernagel, A. Aremu, I. Ashcroft, Using machine learning to aid in the parameter optimisation process for metal-based additive manufacturing, Rapid Prototyp. J. 26 (4) (2019) 625–637.

[151] T. Özel, A. Altay, B. Kaftanoğlu, R. Leach, N. Senin, A. Donmez, Focus variation measurement and prediction of surface texture parameters using machine learning in laser powder bed fusion, J. Manuf. Sci. Eng. 142 (1) (2020).

[152] C. Gobert, E.W. Reutzel, J. Petrich, A.R. Nassar, S. Phoha, Application of supervised machine learning for defect detection during metallic powder bed fusion additive manufacturing using high resolution imaging, Addit. Manuf. 21 (May 2017) (2018) 517–528.

[153] K. Wasmer, In situ quality monitoring in AM using acoustic emission: a reinforcement learning approach, J. Mater. Eng. Perform. 28 (2) (2019) 666–672.